the target cell population once localized to the tumor sites [9]. For targeted ^{10}B delivery in BNCT, immunoliposomes have been employed by linking tumor-targeting ligands to liposome such as antibodies or receptor ligands such as folate [10], transferrin [11] and epidermal growth factor (EGF) [12].

EGFR is a 170-kDa transmembrane tyrosine kinase and the *EGFR* gene is often amplified in human GBMs. EGFRvIII, which has an in-frame deletion of exons 2–7 of the extracellular domain of the *EGFR* gene, is constitutively expressed and amplified in up to 57% of GMBs [13,14]. EGFR is overexpressed in GMB, but is undetectable or weakly expressed in normal brain. Therefore, EGFR is an attractive molecular target for the specific delivery of therapeutic agents to high-grade gliomas [15,16]. An antibody can be directly linked to a liposome through covalent conjugation to a functional group on the liposome [17] or can be post-inserted into a preformed liposome via the micelles of an antibody–lipid conjugate [18,19].

We previously used hollow bionanocapsules (BNCs) composed of modified L protein (the hepatitis B virus surface antigen) for targeting brain tumors [20]. In the present study, BSH was encapsulated into a nickel-liposome and recombinant ZZ-His (IgG Fc-binding motif) was used as an adaptor to conjugate anti-EGFR antibody to the nickel-liposome, resulting in an immunoliposome. Three glioma cell lines, parental U87 glioma cells (PAU87) and human wild-type *EGFR* and *EGFRvIII*-transfected U87 glioma cells (U87 WT and U87 ΔEGFR), were used to evaluate the efficiency with which ^{10}B was delivered by the immunoliposomes *in vitro* and *in vivo*.

2. Materials and methods

2.1. Lipids and chemicals

1,2-Dioleoyl-*sn*-glycero-3-[(*N*-(5-amino-1-carboxypentyl)iminodiacetic acid)-succinyl] nickel (abbreviated as DOGS-NTA-Ni) and the fluorescent analog 25-[*N*-[(7-nitrobenz-2-oxa-1,3-diazol-4-yl)-methyl]amino]-27-norcholesterol (abbreviated as NBD-cholesterol) were purchased from Avanti Polar Lipids (Alabastar, AL). DOPC, DOPG and DSPE-PEG_{2000} were obtained from Nippon Oil and Fats (Tokyo, Japan). BSH ($Na_2B_{12}H_{11}SH$, ^{10}B enriched > 99%) was purchased from Katchem Ltd. (Czechoslovakia). Chloroform, diethyl ether and cholesterol were acquired from Wako Pure Chemicals (Japan).

2.2. Preparation of liposomes

Liposomes composed of DOPC:DOPG:DOGS-NTA-Ni:CH:DSPE-PEG_{2000} (3:3:1:4:0.1, molar ratio) were prepared according to the reverse-phase evaporation (REV) method [11] with slight modification. Briefly, 100 μmol of lipid was dissolved in 2 mL of a chloroform/diethyl ether mixture (1:1 v/v), and 1 mL of a 50 mM BSH solution was added. The ratio of the organic to aqueous phase was 2:1. To prepare liposomes for experiments *in vivo*, a 300 mM BSH solution was used. The mixture was sonicated for 1 min to form a W/O emulsion and evaporated with reduced pressure in a rotary evaporator at 50 °C until a gel was formed. Ten cycles of freezing (dry ice) and thawing (60 °C water bath) were then applied. To obtain liposomes with a homogeneous size distribution, the liposome emulsion was extruded through a polycarbonate membrane 100 nm in pore size using an extruder device at 60 °C. The mean diameter and zeta-potential of the prepared liposomes were determined with an electrophoretic light scattering spectrophotometer (ELS-8000, Photal, Tokyo, Japan). Unencapsulated free BSH was removed by an Amersham sephadex G-50 column (1 × 30 cm). For the preparation of fluorescent liposomes, 1 mol% of NBD-cholesterol was added to the lipid solution.

2.3. Expression and purification of ZZ-His protein

The *ZZ* gene was cloned into pET-22b (+) (Novagen, Madison, WI) and introduced into *E. coli* BL21 (DE3). The expression and purification of ZZ-His were performed as described [21]. Briefly, recombinant proteins were induced by the addition of 1 mM isopropyl-β-D-thiogalatopyranoside (IPTG) when the optical density (OD) of the cell culture at 600 nm reached 0.6. The expressed proteins were purified from the supernatant using ProBond Nickel-chelating resin (Invitrogen) and dialysed against PBS (pH 7.4) at 4 °C for 24 h. The proteins were stored at −80 °C prior to use.

2.4. Cell lines and cell culture

Three human glioma cell lines (kindly donated by Professor Webster K. Cavenee of the University of California at San Diego) were used. U87 ΔEGFR expresses EGFRvIII (145 kDa); U87 WT expresses wild-type EGFR (170 kDa); and PAU87 (parental) expresses no EGFR. The cells were maintained in Dulbecco's modified Eagle's medium (DMEM) (GIBCO) with 10% fetal bovine serum (FBS), penicillin and streptomycin at 37 °C in a humidified atmosphere containing 5% CO_2. Rat primary astrocytes were prepared from a newborn Wistar rat (Japan SLC, Inc.) as described previously [22].

2.5. Antibody-mediated ZZ delivery to EGFR-overexpressing glioma cells

To identify the ability of antibody-directed ZZ-His delivery, we first analyzed the expression level of EGFR in different cells. PAU87, U87 ΔEGFR, and U87 WT cells and primary astrocytes were homogenized by sonication in a boiling buffer containing 1% SDS and Western blotting was carried out as described previously [23]. The blots were probed with an anti-EGFR mouse mAb (101-7300-0, Katayama Chemical Inc., Japan) or the anti-EGFR rat mAb ICR10 (Abcam, Cambridge, UK). After incubation with the appropriate secondary antibody conjugated with horseradish peroxidase (Sigma–Aldrich), positive bands were visualized using an enhanced chemiluminescence detection system (Amersham Biosciences, Pittsburgh, PA).

For delivering ZZ-His into cells via antibody, 18 μg of ZZ-His and anti-EGFR mouse antibody were mixed at a molar ratio of 5 to 1 (ZZ-His to antibody) in 200 μL of PBS (pH 7.4) and rotated at 4 °C for 2 h. Then the ZZ-mAb complex was added to PAU87, U87 ΔEGFR, U87 WT and the primary astrocytes. As a control, only ZZ-His was added. After 2 h of incubation, the cells were washed with PBS twice and treated with 0.025% trypsin to remove surface-binding antibody. They were then resuspended in PBS twice before sonication and subjected to Western blotting using an anti-His (C-term) mouse monoclonal antibody (Invitrogen).

2.6. Analysis of liposome–ZZ–mAb complex (immunoliposome) by ultracentrifugation, Western blotting and lipid measurements

To determine the binding ability of nickel-liposomes and ZZ-His, the two were mixed at a molar ratio of 20–1 (nickel lipid: ZZ-His), rotated at room temperature for 1 h, and then subjected to sucrose gradient ultracentrifugation. Two milliliters of each 10, 20, 30, 40 and 50% sucrose solution was used to prepare the gradient. After 16 h of ultracentrifugation at 35,000 rpm using a Beckman coulter optima-LE-80k ultracentrifuge (rotor SW 41), 1 mL was drawn out and samples were resolved by SDS-PAGE and then transferred to nitrocellulose membranes (Hybond ECL, Amersham Biosciences). Western blotting was performed as described above. The lipid in each fraction was analyzed by the DAOS method using a Phospholipids C reagent kit (Wako Pure Chemical Inc. Ltd., Japan).

For a large amount of immunoliposome, the free ZZ protein was separated by a Sepharose CL-4B column (15 × 70 mm) and the collected liposome–ZZ was concentrated with Amicon Ultra-15 centrifugal filter devices (Millipore). The antibody was conjugated to the liposome–ZZ at a molar ratio of 1 to 20 (mAb:ZZ) and the free antibody was separated with a Sepharose CL-4B column.

2.7. Immunohistochemical analysis (IHC) and measurement of ^{10}B content in vitro

Immunoliposomes were prepared with anti-EGFR rat or mouse mAb for IHC and measuring ^{10}B content, respectively. IHC was carried out to analyze the distribution of ^{10}B *in vitro*. Cells were incubated for 24 h and BSH, liposome, liposome–ZZ, and immunoliposome were added. The final ^{10}B concentration was 1 μg/mL and the antibody concentration was 3 μg/mL. After 3 h of incubation, the cells were washed with PBS twice, fixed with 4% paraformaldehyde (PFA) for 10 min, and then incubated with anti-BSH mouse mAb [24]. The secondary antibody was Cy3-conjugated mouse IgG. Fluorescence signals were observed using a confocal laser microscope (FluoView, Olympus, Japan).

To detect ^{10}B in cells, BSH, liposome, liposome–ZZ, and liposome–ZZ–mAb were added in 6-cm dishes. After 3 h of incubation, the cells were washed with PBS, dissolved in 200 μL of concentrated nitric acid overnight, and diluted with 5 mL of MilliQ water. For liposome–ZZ and immunoliposome-treated cells, 250 mM of imidazole was used for an additional wash to remove surface-bound liposome. The ^{10}B content was measured by inductively coupled plasma-atomic emission spectrometry (ICP-AES, Vista Pro, Seiko Instruments, Japan).

To analyze the effect of the antibody concentration on the delivery of ^{10}B, 1 mM of liposome was incubated with U87 ΔEGFR cells in the presence of 0.1, 0.5, 1, 3, 5, 10, or 50 μg/mL of mAb for 3 h. To analyze the effect of time on the delivery, 3 μg/mL of antibody was used and U87 ΔEGFR cells were incubated with 1 mM of immunoliposome for 1, 3, 5, 7, 12 and 24 h. The ^{10}B measurements were carried out as described above.

2.8. Brain tumor model and detection of immunoliposomes in vivo

U87 ΔEGFR cells (5×10^5 cells/5 μL) were injected into the striatum of female 4-to-6 week-old nude mice (15-20 g, BALB/c Slc-nu/nu; Japan SLC) as described [24]. After two weeks, 400 μL of NBD-liposome and NBD-immunoliposome was administered into tumor-bearing mice intravenously via the tail. After 4 h and 24 h, the mice were sacrificed and the brains were placed in PBS. Sections of 10-μm thickness were cut on a microtome (CM 1850, Leica Microsystems, Wetzlar, Germany). IHC was

Please cite this article in press as: Feng B et al., Delivery of sodium borocaptate to glioma cells using immunoliposome conjugated with anti-EGFR antibodies by ZZ-His, Biomaterials (2009), doi:10.1016/j.biomaterials.2008.12.010

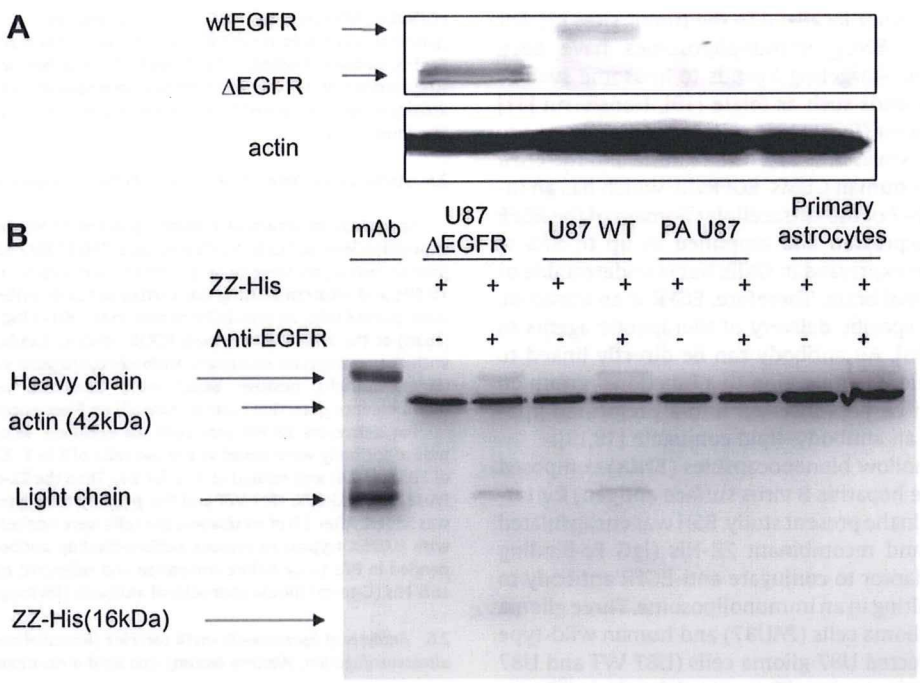

Fig. 1. EGFR expression level in different cell lines and antibody-mediated ZZ-His delivery. (A) Cell lysates of primary astrocytes and glioma cell lines U87 ΔEGFR, U87 WT, and PAU87 were subjected to 6% SDS-PAGE and transferred to PVDF membranes. Anti-EGFR mouse monoclonal antibody was used for detection of the wild-type and vIII EGFR. (B) ZZ–mAb and ZZ were incubated with cells for 2 h and the delivered proteins were detected by anti-His mouse mAb.

carried out as described above. The fluorescence labeling of liposomes was observed immediately after the sections were prepared.

For the analysis of the distribution of ^{10}B, immunoliposomes and liposomes were injected via the tail at a dose of 35 mg ^{10}B/kg. Tumor, normal brain, liver, and blood were sampled at 4, 12, 24, and 48 h post-administration, and the samples were digested with a nitric acid solution overnight and diluted with MillQ water for ICP-AES.

2.9. Statistical analysis

Data are shown as the mean ± S.E. Data were analyzed using Student's *t*-test to compare the two conditions, and $p < 0.05$ was considered significant.

3. Results

3.1. Antibody-mediated delivery of ZZ into glioma cells

EGFR levels in each cell line were determined by Western blotting using an anti-EGFR monoclonal antibody (mAb). The mAb detected EGFR in ΔEGFR-expressing U87 cells (U87 ΔEGFR) and wild-type EGFR-expressing cells (U87 WT) (Fig. 1A). In contrast, EGFR expression was undetectable in PAU87 cells and primary astrocytes. Thereafter, we examined the ability of the mAb to target EGFR-overexpressing glioma cells. The Western blotting showed that the mAb and ZZ-His were detected in U87 ΔEGFR and U87 WT cells when ZZ was bound with the antibody (Fig. 1B). In contrast, neither mAb nor ZZ-His was detected without conjugation with the anti-EGFR mAb (Fig. 1B). Moreover, no antibody or ZZ was detected in PAU87 cells and primary astrocytes (Fig. 1B). These results suggest that the anti-EGFR mAb is capable of targeting glioma cells expressing wild-type and vIII EGFR.

3.2. Identification of liposome–ZZ–mAb complex

When 10 mol% of DOGS-NTA-Ni and 1 mol% of DSPE-PEG_{2000} were used in the liposome formulation, no aggregation occurred. It was reported that NTA-Ni increased the sensitivity and DSPE-PEG_{2000} reduced the aggregation [25]. Therefore, to identify the ability of ZZ-His to bind with mAb and nickel-liposomes containing 10 mol% DOGS-NTA-Ni and 1 mol% DSPE-PEG_{2000}, we carried out ultracentrifugation and Western blot analyses. The ultracentrifugation indicated that the nickel-liposomes bound with ZZ-His effectively. The positions in different layers are shown in Fig. 2A. When 1 mol% DSPE-PEG_{2000} was used in the liposome, the distribution was the same as that without DSPE-PEG_{2000} (data not shown). As shown in Fig. 2B, most of the PEG-liposomes were in the first layer after ultracentrifugation. When ZZ-His was mixed with the nickel-liposome and mAb, the liposomes occurred in the fourth and fifth layers. Results of Western blotting in Figs. 2C–F show that the ZZ, liposome, and antibody are all in the same layer (fractions 4 and 5), while free ZZ-His and mAb are in the first and third fractions, respectively. These results suggest that mAb is effectively bound to liposome via ZZ adaptor. When the molar ratio of nickel lipid to ZZ was 20:1, about half of the ZZ bound with liposomes (Fig. 2D). The ratio was adjusted to 40:1 in the subsequent experiment.

The Western blotting and lipid analysis also indicated that the binding of the nickel-liposome to ZZ and of ZZ to the mAb was specific because the liposome showed no ability to bind ZZ when nickel lipid was not used (data not shown). When ZZ was not used, the nickel-liposome showed no binding with mAb (data not shown). A scheme of the immunoliposome is shown in Fig. 3A. The diameter of the liposome is about 100 nm, but when ZZ and mAb are added, the diameter of the immunoliposome increases to 130 nm (Fig. 3B). The *z*-potential also increases, from −44.74 to −24.67 mV (Fig. 3C). The immunoliposomes were used for *in vivo* experiments.

3.3. Delivery of BSH into glioma cells in vitro

We examined the effect of the immunoliposomes on the delivery of ^{10}B in different cell lines. The cells were incubated with the immunoliposomes for 3 h and the delivery of ^{10}B was then investigated with IHC using the anti-BSH mAb (Fig. 4). BSH was not

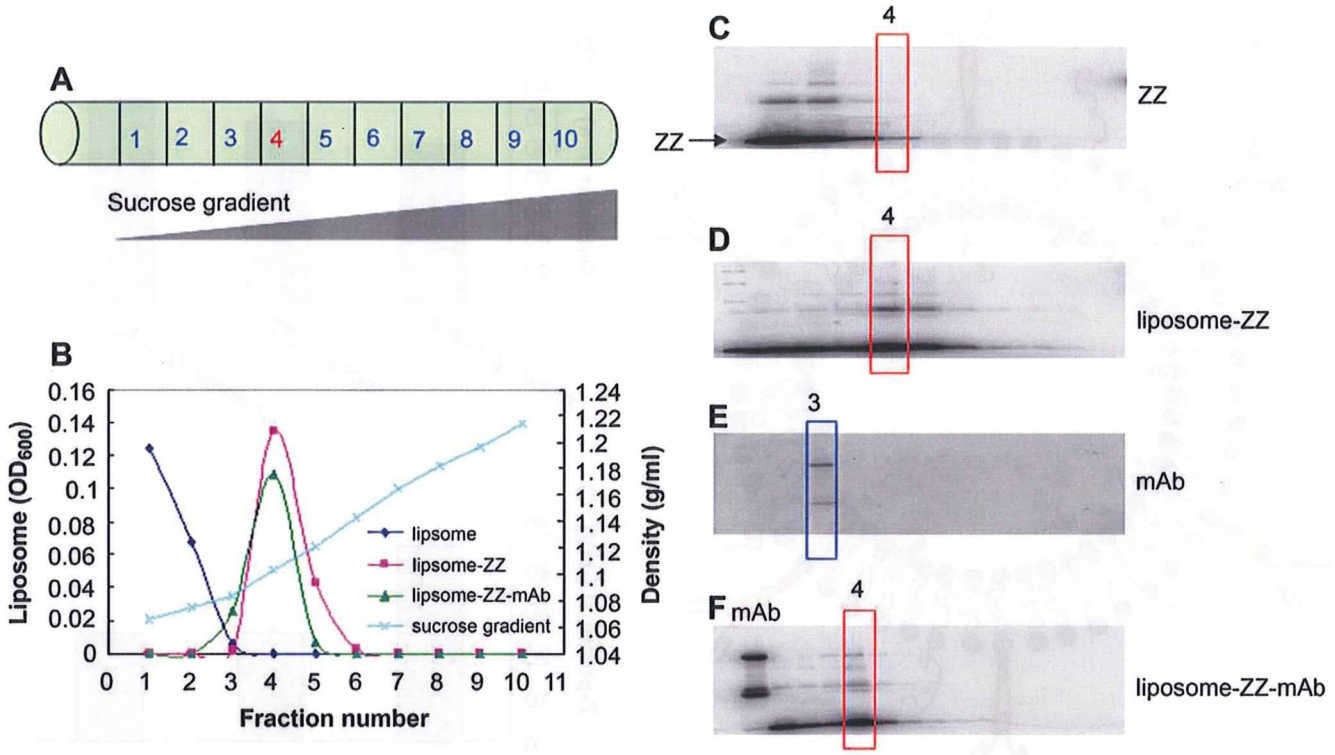

Fig. 2. Analysis of the liposome–ZZ–mAb complex. (A) Distribution of each fraction in a sucrose gradient. (B) Phospholipids in different fractions were measured by the DAOS method after ultracentrifugation and absorbance at OD_{600} was used to indicate the position of liposomes. (C, D) The position of ZZ was identified by anti-His antibody after ultracentrifugation in ZZ and liposome-ZZ samples. (E, F) The positions of mAb and ZZ were identified by anti-His antibody after ultracentrifugation in mAb and liposome–ZZ–mAb samples.

detected in primary astrocytes and only a small amount of BSH was delivered into PAU87 cells (Fig. 4). The results of ICP-AES were consistent with those of IHC (data not shown). In contrast, BSH was delivered in almost all U87 ΔEGFR and U87 WT cells expressing vIII EGFR and wild-type EGFR, respectively (Fig. 4). To demonstrate that BSH was actually present inside glioma cells and to exclude the possibility that it was just attached to the surface of the cells, serial optical sections of 2 μm taken along the *Z*-dimension of the immunostained cells were collected with a confocal microscope (Supplementary material). Signal for BSH on the surface of the cells was weak and most BSH was observed in the cells (Supplementary material). Moreover, strong signals were observed in the nucleus. To further investigate whether BSH delivered by immunoliposomes functions as ^{10}B in glioma cells, ICP-AES was performed (Fig. 5A). In U87 ΔEGFR and U87 WT cells incubated with control liposomes without the anti-EGFR antibody, the ^{10}B level was low. In contrast, a high level of ^{10}B was detected in the cells incubated with immunoliposomes (Fig. 5A). Moreover, immunoliposomes did not deliver ^{10}B into PAU87 cells (Fig. 5A). These results suggest that immunoliposomes conjugated with anti-EGFR antibodies efficiently deliver ^{10}B in glioma cells expressing EGFR.

3.4. Effect of antibody concentration and time course on BSH delivery

We examined the dose-dependent effect of the antibody on the efficiency of ^{10}B delivery. Following 3 h of incubation with immunoliposomes in the presence of 0.1, 0.5, 1, 3, 5, 10, or 50 μg/mL of anti-EGFR antibody, the cells were washed twice with PBS containing Ni-chelating components (250 mM imidazole) to remove surface-bound liposomes. ICP-AES revealed that 0.5 μg/mL of antibody was effective for the delivery of ^{10}B compared with liposomes without the antibody (Fig. 5B). In the time-course experiment, 3 μg/mL of antibody was used for the detection of ^{10}B and cells were incubated with immunoliposomes for 1, 3, 5, 7, 12 and 24 h. The ^{10}B content of cells increased with time (Fig. 5C). When cells were incubated with immunoliposomes at 4 °C, little ^{10}B was detected inside them (data not shown), suggesting that the uptake of immunoliposomes was temperature-dependent and the immunoliposomes were internalized into cells by endocytosis.

3.5. In vivo delivery of BSH in brain tumor by immunoliposomes

To observe the distribution of the liposome and BSH *in vivo*, we injected NBD-liposomes and NBD-immunoliposomes into the tail of nude mice two weeks at the tumor engraftment. In freshly prepared brain slices, fluorescence could be seen in the tumor and blood vessel wall 4 h after the injection (Figs. 6A and D). In normal tissues, strong fluorescence was seen only in the blood vessel wall (arrowheads in Fig. 6E). In the NBD-liposome-injected mice, no fluorescence was seen in the tumor (Fig. 6G). Signal's distribution indicates that the immunoliposomes were delivered into the tumor via the blood stream, and the delivery was antibody-dependent. BSH's distribution was examined by IHC using the anti-BSH mAb. BSH was clearly detected in the tumor whereas it was undetectable in normal tissue (Figs. 7A and B). A low level of BSH was observed in both tumor and normal tissues of the mice treated with the control liposome without conjugation of the anti-EGFR mAb (Figs. 7D and E). In immunoliposome-treated mice for 24 h, BSH was detected in the tumor and surrounding regions (Fig.7G and H).

We finally compared ^{10}B content among each tissue in this model of brain tumors. Immunoliposomes effectively delivered BSH to tumors compared with liposomes (Fig. 8). In immunoliposome-treated mice, the amount of ^{10}B in the tumor reached

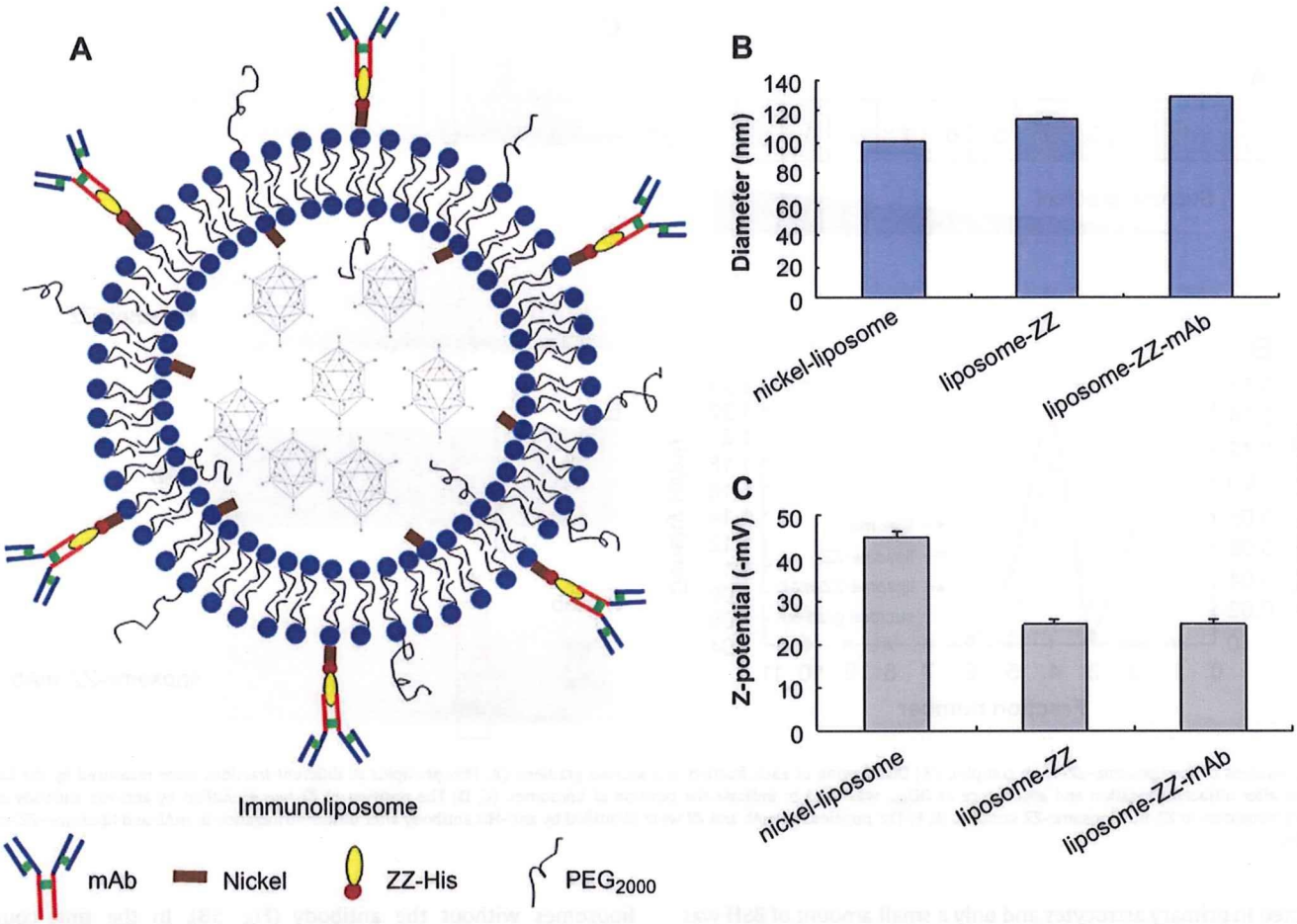

Fig. 3. Characteristics of the immunoliposomes. (A) Scheme of components of the immunoliposome. (B, C) Diameter and z-potential of the nickel-liposome, liposome–ZZ and immunoliposome.

28.36 ± 7.63 μg/g 24 h after the injection and remained high until the 48 h mark (21.38 ± 5.31 μg/g). In liposome-treated samples, on the other hand, the ^{10}B content of tumors at 24 and 48 h was 3.45 and 2.97 μg/g, respectively (Fig. 8A). In normal brain tissue of the mice treated with immunoliposomes and liposomes, ^{10}B content was low at all time points (Fig. 8B). In liver, ^{10}B levels peaked 12 h after the injection and then decreased in a time-dependent manner (Fig. 8C). In blood, ^{10}B levels reached a maximum 4 h after the injection of immunoliposomes and rapidly decreased 12 h after the injection (Fig. 8D).

4. Discussion

The aim of the present study was to develop a novel ^{10}B delivery system for targeting glioma cells. Since the appearance of BNCT in the 1950s, different methods of delivering ^{10}B into tumor cells have been investigated [2,4], though only BSH and BPA have been used clinically. BSH is thought to penetrate tumor tissue through a disrupted blood–brain barrier (BBB) and thus accumulates little in normal brain tissue [26]. BPA is an analog of an essential amino acid (tyrosine) and is actively taken up by tumor cells but also accumulates measurably in normal brain [5]. The specific accumulation of ^{10}B in tumor tissue is still a limitation to the use of this technology. In the present study, we encapsulated BSH in liposomes and used a universal adaptor (ZZ) to conjugate an anti-EGFR mAb to target glioma cells.

The wild-type EGFR and its isoforms (variant III) are considered prime targets for the specific delivery of a variety of diagnostic and therapeutic agents [9,27,28]. In BNCT, mAb or EGF-conjugated immunoliposomes and boronated mAb have been used to deliver ^{10}B into glioma cells [7,12,14,29]. The anti-EGFR antibody used in this study recognized both wild-type and vIII EGFR, so ZZ-His bound with the mAb could be effectively delivered into EGFR-overexpressing glioma cells. In our ^{10}B delivery system, the ability of ZZ to bind the nickel-liposome was not affected by the addition of 1% DSPE-PEG_{2000} and the liposome–ZZ complex showed the same position as the naked nickel-liposome–ZZ after ultracentrifugation (data not shown). Chikh et al. [30] reported that the addition of 5 mol% of DSPE-PEG_{2000} caused a slight change in the rate of binding, but the incorporation efficiency of His-tagged peptide did not change. The binding of DOGS-NTA-Ni with ZZ-His is not achieved at a theoretical ratio. When a molar ratio of 20:1 (DOGS-NTA-Ni:ZZ-His) was used, only about half the amount of ZZ could be conjugated with the liposome, and the liposome–ZZ complex was in the fourth layer (Fig. 2D). When the ratio was adjusted to 40:1, no free ZZ was detected by Western blotting after ultracentrifugation (data not shown). The interaction of DOGS-NTA-Ni with His-tags has been reported to be stronger than or equivalent to that of antibody interactions (10^{-6} to 10^{-9} M), with a dissociation constant (k_d) in the range of 10^{-6} to 10^{-13} M at pH 7–8 depending on the protein and location of the His-tag on the protein [31,32]. When the molar ratio of ZZ to mAb was 25:1, all the liposome–ZZ–mAb complexes occurred in the four and fifth layers after ultracentrifugation. For the preparation of immunoliposomes, removal of free ZZ and mAb from the liposome–ZZ complex may be important, because free mAb or ZZ–mAb will bind to EGFR-overexpressing cells.

Please cite this article in press as: Feng B et al., Delivery of sodium borocaptate to glioma cells using immunoliposome conjugated with anti-EGFR antibodies by ZZ-His, Biomaterials (2009), doi:10.1016/j.biomaterials.2008.12.010

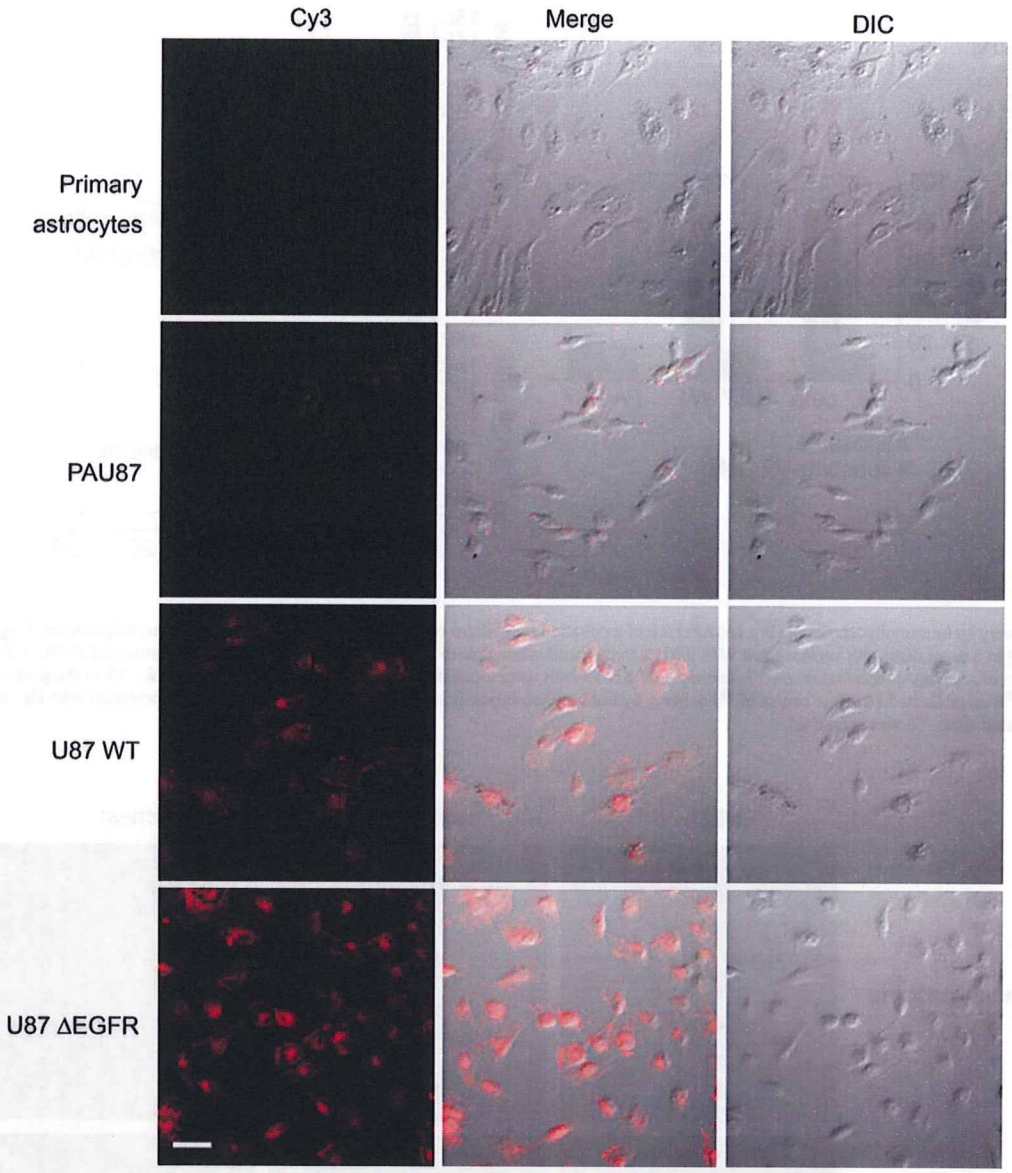

Fig. 4. Analysis by immunohistochemistry (IHC) of ^{10}B delivery by immunoliposomes in different cell lines. Immunoliposomes (liposome: 1 mM; anti-EGFR rat mAb: 3 μg/mL; ^{10}B: 1 μg/mL) were incubated with primary astrocytes, PAU87, U87 WT and U87 ΔEGFR for 3 h and fixed with 4% PFA. Anti-BSH mouse mAb was used as the primary antibody and Cy3-conjugated mouse IgG was used as the secondary antibody. The fluorescence signals were visualized using a confocal laser microscope. Bar = 50 μm.

The conjugation of ZZ-His protein at the surface of a liposome by DOGS-NTA-Ni will make the liposome more stable in blood. Moreover, the combination of ZZ and PEG inhibits interaction of the liposome and cells to some degree, and so inhibits non-specific endocytosis. Recently, NTA-Ni has been reported to attach His-tag peptides and proteins to the liposome [30]. van Broekhoven et al. [33] used NTA-Ni for surface mobilization of His-tagged antibodies for DC-specific receptor to DCs.

An advantage of using ZZ to bind with Fc of IgG is that complete-IgG-labeled liposomes may have shorter circulation times, due to the rapid identification and uptake of the Fc fragment by macrophages in circulation [34]. Allen et al. [35] reported that increasing the density of liposome-grafted antibodies resulted in a faster clearance of immnoliposomes from the circulation. To overcome this, an antibody fragment (Fab′ and scFV) that lacks the Fc portion was used, and showed identical circulation times with PEGylated non-immunolabeled liposome when conjugated to the free termini of PEGylated lipid [27].

Protein A has been widely used for purifying IgG because of its specific binding to the Fc domain of IgG through bioaffinity [36]. In this study, we used the ZZ motif (Fc-binding domain) as an adaptor to conjugate an antibody to the liposome, resulting in an immunoliposome. In this ^{10}B delivery system, the specificity and totality of the antibody are retained, and not affected by thiolation of the antibody during liposome's preparation. The His-tag at the C-terminus of ZZ is used not only for purification, but also for interaction with chelated divalent metal ions, nickel in the NTA-Ni lipid [37]. NTA forms a strong complex with four of the metal sites, leaving two additional sites for interaction with the His-tag present on the protein. After incubation in medium for 12 h, the immunoliposomes still deliver ^{10}B efficiently (data not shown), indicating the stability of liposome–ZZ–mAb in serum. Long-term stability of the immunoliposomes in serum will permit high levels of ^{10}B to accumulate in tumor cells *in vivo*.

Gliomas have a poor prognosis due to their exceptional ability to infiltrate normal brain tissue, often along blood vessels or nerve

Please cite this article in press as: Feng B et al., Delivery of sodium borocaptate to glioma cells using immunoliposome conjugated with anti-EGFR antibodies by ZZ-His, Biomaterials (2009), doi:10.1016/j.biomaterials.2008.12.010

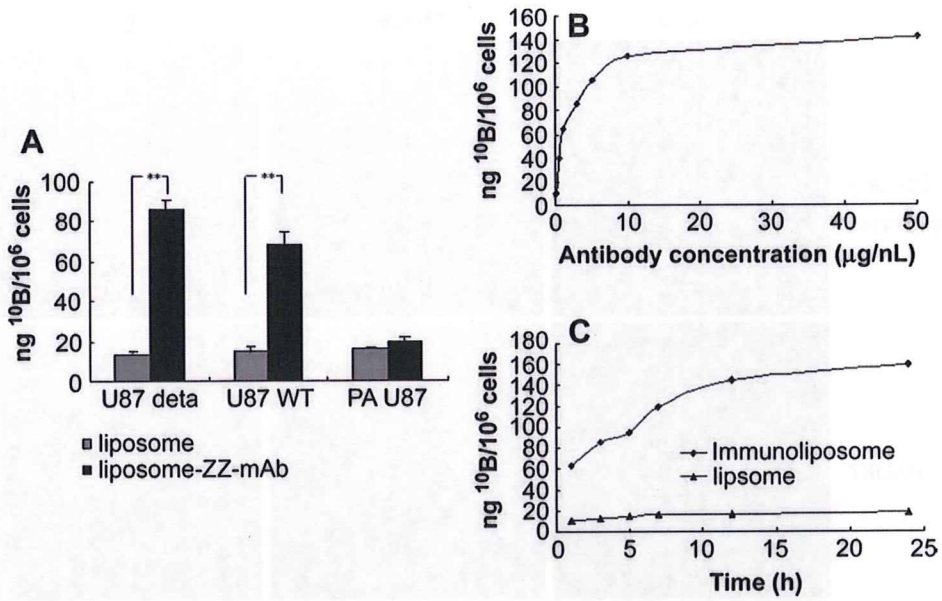

Fig. 5. ICP-AES of ^{10}B delivery by immunoliposomes *in vitro*. (A) After 3 h of incubation in medium containing 1 mM of liposomes or immunoliposomes (1 μg/mL of ^{10}B and 3 μg/mL of anti-EGFR mouse mAb) in a 6-cm dish, cells were treated with 0.025% trypsin and washed with 250 mM of imizadole and PBS, and amounts of internalized ^{10}B were detected. $n = 4$; ** $p < 0.01$. (B) Effect of antibody concentration on ^{10}B delivery. U87 ΔEGFR cells were incubated with 1 mM of immunoliposomes for 3 h in the presence of 0.1, 0.5, 1, 3, 5, 10, or 50 μg/mL of mAb and ^{10}B was detected. (C) Time course of ^{10}B delivery by immunoliposomes. Immunolipoosmes and lipsomes were incubated with U87 ΔEGFR cells for 1, 3, 5, 7, 12 and 24 h. At the indicated time, ^{10}B was measured.

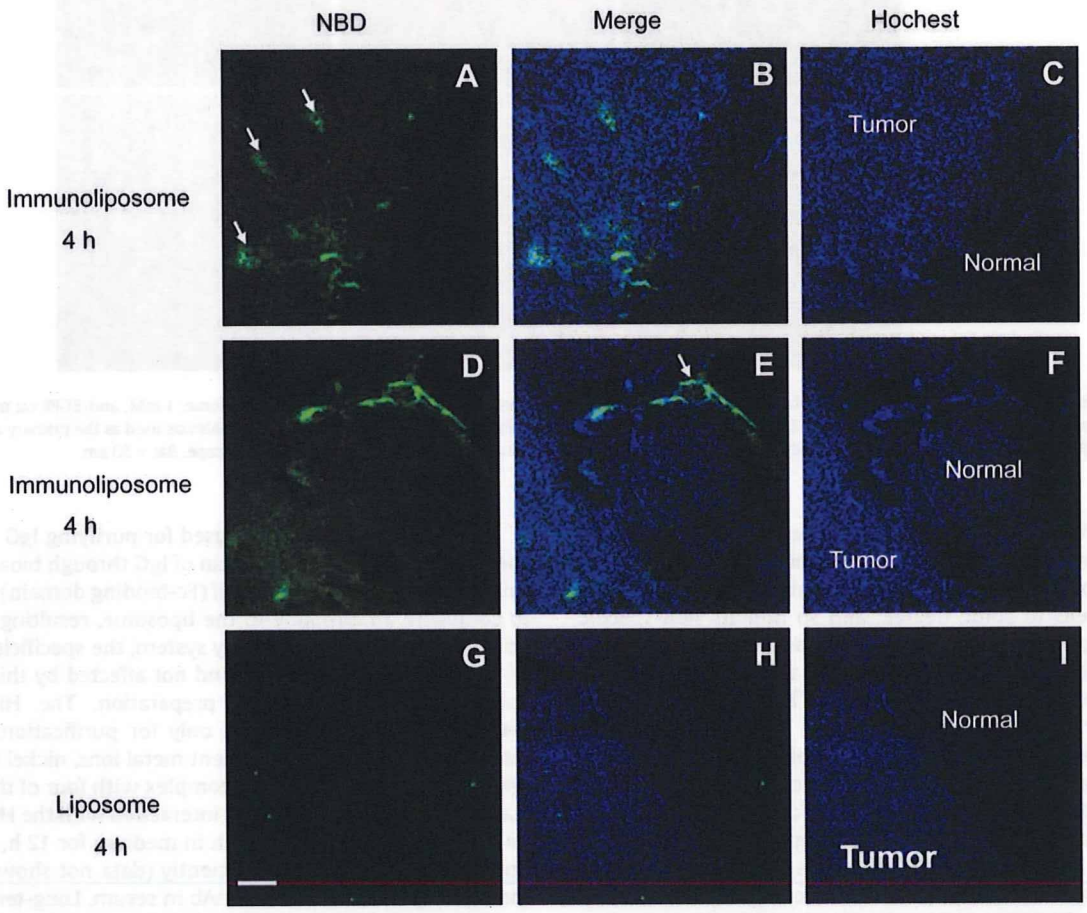

Fig. 6. Distribution *in vivo* of NBD-immunoliposomes. Four hundred microliters (liposome concentration: 50 mM; antibody concentration: 180 μg/mL) of NBD-immunoliposome or NBD-liposome was injected via the tail into nude mice two weeks after tumor engraftment. Green fluorescence of NBD and blue fluorescence of hochest were used to indicate the positions of the liposomes and tumor 4 h after injection, respectively. (A,D,G) NBD-fluorescence images (10×) of freshly prepared brain slices. (C,F,I) Hochest-fluorescence images (10×) of freshly prepared brain slices. (B,E,H) Merging of the NBD and hochest signals. Arrows indicate the positions of blood vessels. Bar = 200 μm.

Please cite this article in press as: Feng B et al., Delivery of sodium borocaptate to glioma cells using immunoliposome conjugated with anti-EGFR antibodies by ZZ-His, Biomaterials (2009), doi:10.1016/j.biomaterials.2008.12.010

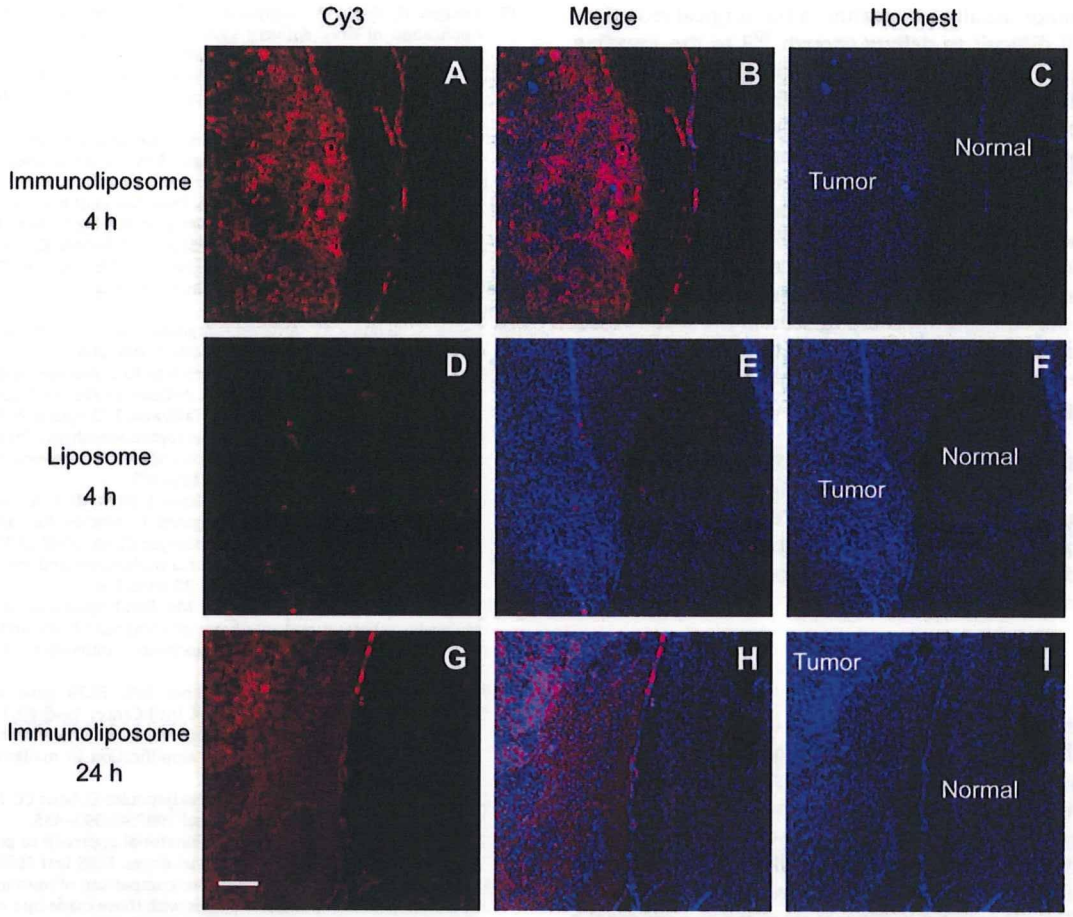

Fig. 7. IHC analysis of BSH's distribution *in vivo*. Four hundred microliters of immunoliposomes or liposomes was injected into the tail of nude mice two weeks after tumor engraftment. Slices were prepared 4 and 24 h post-injection. Anti-BSH mouse mAb and Cy3-conjugated mouse IgG were used as the primary and secondary antibody. Red fluorescence of Cy3 was used to show the distribution of BSH and blue fluorescence of hochest was used to indicate the position of the tumor. (A,D,G) Cy3-fluorescence images (10×). (C,F,I) Hochest-fluorescence images (10×). (B,E,H) Merging of the Cy3 and hochest signals. Bar = 200 μm.

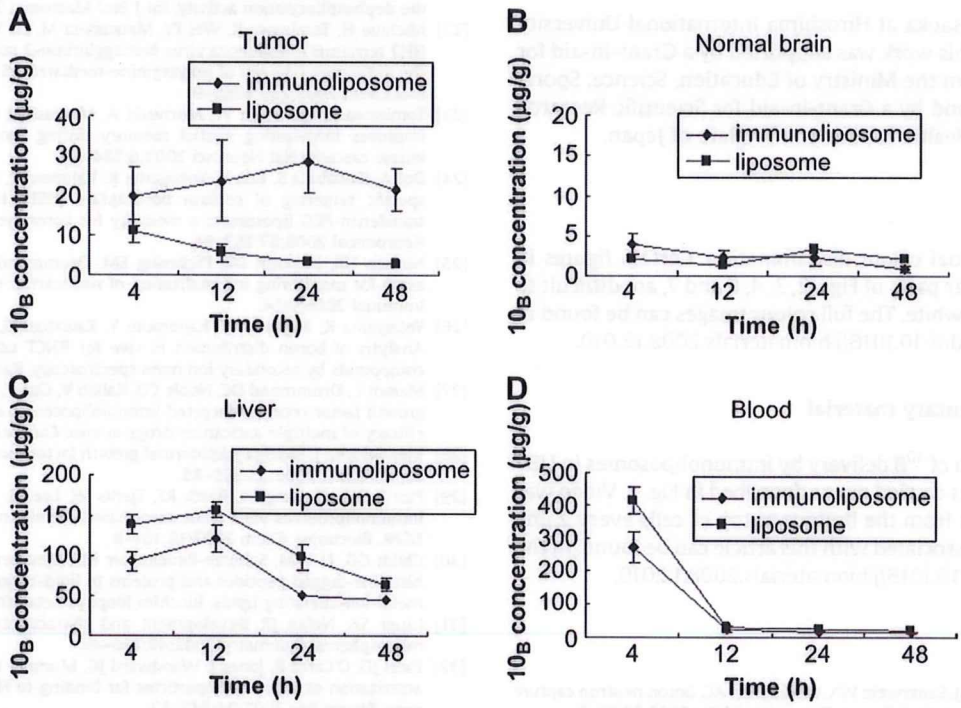

Fig. 8. Time course of ^{10}B's distribution *in vivo*. ^{10}B concentrations in tumor (A), normal brain (B), liver (C) and blood (D) were measured after 400 μL of immunoliposome or liposome was injected into tumor-bearing mice via a tail vein at a dose of 35 mg ^{10}B/kg.

Please cite this article in press as: Feng B et al., Delivery of sodium borocaptate to glioma cells using immunoliposome conjugated with anti-EGFR antibodies by ZZ-His, Biomaterials (2009), doi:10.1016/j.biomaterials.2008.12.010

fibers [38]. The tumor usually recurs after initial surgical resection. In BNCT, it is still difficult to deliver enough ^{10}B to the invading glioma cells in the brain. Our immunoliposomes may solve this problem. PEG-lipid and ZZ on the surface of the liposome provide steric stabilization and prolong circulation time. In solid tumors, the BBB is destroyed, and the abnormal tumor vessels are discontinuous, with pores varying from 100 to 780 nm [39,40]. At 4 h after an intravenous injection, the immunoliposome reached the tumor through the blood stream, and the anti-EGFR mAb effectively recognized the EGFR on the surface of tumor cells. The immunoliposomes had passed through the tumor vessel and penetrated tumor cells, as weak fluorescence could be seen in the blood vessel wall (Fig. 6A). At normal sites, we could see strong fluorescence on the surface of vessel walls and no fluorescence in normal tissues (Fig. 6E). This suggests that the immunoliposomes could not pass through the BBB in normal tissue.

To avoid possible toxic effects of DOGS-NTA-Ni, we are now exploring a new way to conjugate ZZ to the liposome surface. Our immunoliposomes can be used as a universal drug delivery system to deliver other anti-cancer drugs to tumor cells if we know the receptor or ligand on the surface of the tumor cells. In this study, ^{10}B delivery has been proved effective.

5. Conclusion

The results described above support the use of immunoliposomes to specifically deliver BSH to glioma cells. Recombinant ZZ-His (Fc-binding domain) was conjugated to liposomes containing 10 mol% DOGS-NTA-Ni and 1 mol% DSPE-PEG_{2000} to prepare immunoliposomes. This is the first time that an antibody-binding domain has been used to deliver ^{10}B in BNCT. ICP-AES and IHC indicated that ^{10}B was specifically delivered into EGFR-overexpresing glioma cells *in vitro* and *in vivo*. Thus, it appears that our system can be used for the specific delivery of other anti-cancer drugs.

Acknowledgements

We thank Dr. S. Kasaoka at Hiroshima International University for technical advice. This work was supported by a Grant-in-aid for Scientific Research from the Ministry of Education, Science, Sports and Culture of Japan and by a Grant-in-aid for Scientific Research from the Ministry of Health, Labour and Welfare of Japan.

Appendix

Figures with essential colour discrimination. Certain figures in this article, in particular parts of Figs. 2, 3, 4, 6 and 7, are difficult to interpret in black and white. The full colour images can be found in the online version, at doi:10.1016/j.biomaterials.2008.12.010.

Appendix. Supplementary material

Z-Dimensional scan of ^{10}B delivery by immunoliposomes in U87 ΔEGFR (100×). IHC was carried out as described in Fig. 4. Video was recorded at *Z*-sections from the bottom to top of cells every 2 μm. Supplementary data associated with this article can be found, in the online version, at doi:10.1016/j.biomaterials.2008.12.010.

References

[1] van Rij CM, Wilhelm AJ, Sauerwein WA, van Loenen AC. Boron neutron capture therapy for glioblastoma multiforme. Pharm World Sci 2005;27:92–5.
[2] Mehta SC, Lu DR. Targeted drug delivery for boron neutron capture therapy. Pharm Res 1996;13:344–51.
[3] Yanagië H, Ogata A, Sugiyama H, Eriguchi M, Takamoto S, Takahashi H. Application of drug delivery system to boron neutron capture therapy for cancer. Expert Opin Drug Deliv 2008;5:427–43.
[4] Barth RF, Coderre JA, Vicente MG, Blue TE. Boron neutron capture therapy of cancer: current status and future prospects. Clin Cancer Res 2005;11:3987–4002.
[5] Yokoyama K, Miyatake S, Kajimoto Y, Kawabata S, Doi A, Yoshida T, et al. Pharmacokinetic study of BSH and BPA in simultaneous use for BNCT. J Neurooncol 2006;78:227–32.
[6] Soloway AH, Hatanaka H, Davis MA. Penetration of brain and brain tumor. VII. Tumor-binding sulfhydryl boron compounds. J Med Chem 1967;10:714–7.
[7] Carlsson J, Kullberg EB, Capala J, Sjöberg S, Edwards K, Gedda L. Ligand liposomes and boron neutron capture therapy. J Neurooncol 2003;62:47–59.
[8] Hawthorne MF, Shelly K. Liposomes as drug vehicles for boron agents. J Neurooncol 1997;33:53–8.
[9] Sofou S, Sgouros G. Antibody-targeted liposomes in cancer therapy and imaging. Expert Opin Drug Deliv 2008;5:189–204.
[10] Pan XQ, Wang H, Lee RJ. Boron delivery to a murine lung carcinoma using folate receptor-targeted liposomes. Anticancer Res 2002;22:1629–33.
[11] Maruyama K, Ishida O, Kasaoka S, Takizawa T, Utoguchi N, Shinohara A, et al. Intracellular targeting of sodium mercaptoundecahydrododecaborate (BSH) to solid tumors by transferrin-PEG liposomes, for boron neutron-capture therapy (BNCT). J Control Release 2004;98:195–207.
[12] Bohl Kullberg E, Bergstrand N, Carlsson J, Edwards K, Johnsson M, Sjöberg S, et al. Development of EGF-conjugated liposomes for targeted delivery of boronated DNA binding agents. Bioconjug Chem 2002;13:737–43.
[13] Friedman HS, Bigner DD. Glioblastoma multiforme and the epidermal growth factor receptor. N Engl J Med 2005;353:1997–9.
[14] Yang W, Wu G, Barth RF, Swindall MR, Bandyopadhyaya AK, Tjarks W, et al. Molecular targeting and treatment of composite EGFR and EGFRvIII-positive gliomas using boronated monoclonal antibodies. Clin Cancer Res 2008;14:883–91.
[15] Schwechheimer K, Huang S, Cavenee WK. EGFR gene amplification-rearrangement in human glioblastomas. Int J Cancer 1995;62:145–8.
[16] Sauter G, Maeda T, Waldman FM, Davis RL, Feuerstein BG. Patterns of epidermal growth factor receptor amplification in malignant gliomas. Am J Pathol 1996;148:1047–53.
[17] Park JW, Hong K, Kirpotin DB, Papahadjopoulos D, Benz CC. Immunoliposomes for cancer treatment. Adv Pharmacol 1997;40:399–435.
[18] Ishida T, Iden DL, Allen TM. A combinatorial approach to producing sterically stabilized (Stealth) immunoliposomal drugs. FEBS Lett 1999;460:129–33.
[19] Iden DL, Allen TM. *In vitro* and *in vivo* comparison of immunoliposomes made by conventional coupling techniques with those made by a new post-insertion approach. Biochim Biophys Acta 2001;1513:207–16.
[20] Tsutsui Y, Tomizawa K, Nagita M, Michiue H, Nishiki T, Ohmori I, et al. Development of bionanocapsules targeting brain tumors. J Control Release 2007;122:159–64.
[21] Feng B, Zhao CH, Tanaka S, Imanaka H, Imamura K, Nakanishi K. TPR domain of Ser/Thr phosphatase of *Aspergillus oryzae* shows no auto-inhibitory effect on the dephosphorylation activity. Int J Biol Macromol 2007;41:281–5.
[22] Michiue H, Tomizawa K, Wei FY, Matsushita M, Lu YF, Ichikawa T, et al. The NH2 terminus of influenza virus hemagglutinin-2 subunit peptides enhances the antitumor potency of polyarginine-mediated p53 protein transduction. J Biol Chem 2005;280:8285–9.
[23] Tomizawa K, Iga N, Lu YF, Moriwaki A, Matsushita M, Li ST, et al. Oxytocin improves long-lasting spatial memory during motherhood through MAP kinase cascade. Nat Neurosci 2003;6:384–90.
[24] Doi A, Kawabata S, Iida K, Yokoyama K, Kajimoto Y, Kuroiwa T, et al. Tumor-specific targeting of sodium borocaptate (BSH) to malignant glioma by transferrin-PEG liposomes: a modality for boron neutron capture therapy. J Neurooncol 2008;87:287–94.
[25] Nielsen UB, Kirpotin DB, Pickering EM, Drummond DC, Marks JD. A novel assay for monitoring internalization of nanocarrier coupled antibodies. BMC Immunol 2006;7:24.
[26] Yokoyama K, Miyatake S, Kajiomoto Y, Kawabata S, Doi A, Yoshida T, et al. Analysis of boron distribution *in vivo* for BNCT using two different boron compounds by secondary ion mass spectroscopy. Radiat Res 2007;167:102–9.
[27] Mamot C, Drummond DC, Noble CO, Kallab V, Guo Z, Hong K, et al. Epidermal growth factor receptor-targeted immunoliposomes significantly enhance the efficacy of multiple anticancer drugs *in vivo*. Cancer Res 2005;24:11631–8.
[28] Mendelsohn J, Baselga J. Epidermal growth factor receptor targeting in cancer. Semin Oncol 2006;33:369–85.
[29] Pan X, Wu G, Yang W, Barth RF, Tjarks W, Lee RJ. Synthesis of cetuximab-immunoliposomes via a cholesterol-based membrane anchor for targeting of EGFR. Bioconjug Chem 2007;18:101–8.
[30] Chikh GG, Li WM, Schutze-Redelmeier MP, Meunier JC, Bally MB. Attaching histidine-tagged peptides and proteins to lipid-based carriers through use of metal-ion-chelating lipids. Biochim Biophys Acta 2002;1567:204–12.
[31] Lauer SA, Nolan JP. Development and characterization of Ni-NTA-bearing microspheres. Cytometry 2002;48:136–45.
[32] Patel JD, O'Carra R, Jones J, Woodward JG, Mumper RJ. Preparation and characterization of nickel nanoparticles for binding to His-tag proteins and antigens. Pharm Res 2007;24:343–52.
[33] van Broekhoven CL, Parish CR, Demangel C, Britton WJ, Altin JG. Targeting dendritic cells with antigen-containing liposomes: a highly effective

procedure for induction of antitumor immunity and for tumor immunotherapy. Cancer Res 2004;64:4357–65.
[34] Kamps JA, Scherphof GL. Receptor versus non-receptor mediated clearance of liposome. Adv Drug Deliv Rev 1998;32:81–97.
[35] Allen TM, Brandeis E, Hansen CB, Kao GY, Zalipsky S. A new strategy for attachment of antibodies to sterically stabilized liposome resulting in efficient targeting to cancer-cells. Biochim Biophys Acta 1995;1237:99–108.
[36] Moks T, Abrahmsén L, Nilsson B, Hellman U, Sjöquist J, Uhlén M. Staphylococcal protein A consists of five IgG-binding domains. Eur J Biochem 1986;156:637–43.
[37] Hochuli E, Döbeli H, Schacher A. New metal chelate adsorbent selective for proteins and peptides containing neighbouring histidine residues. J Chromatogr 1987;411:177–84.
[38] Laerum OD, Bjerkvig R, Steinsvåg SK, de Ridder L. Invasiveness of primary brain tumors. Cancer Metastasis Rev 1984;3:223–36.
[39] Maruyama K, Takahashi N, Tagawa T, Nagaike K, Iwatsuru M. Immunoliposomes bearing polyethyleneglycol-coupled Fab' fragment show prolonged circulation time and high extravasation into targeted solid tumors *in vivo*. FEBS Lett 1997;413:177–80.
[40] Siwak DR, Tari AM, Lopez-Berestein G. The potential of drug-carrying immunoliposomes as anticancer agents. Clin Cancer Res 2002;8:955–6.

Please cite this article in press as: Feng B et al., Delivery of sodium borocaptate to glioma cells using immunoliposome conjugated with anti-EGFR antibodies by ZZ-His, Biomaterials (2009), doi:10.1016/j.biomaterials.2008.12.010

定位的放射線治療
13：23～30, 2009

ホウ素中性子捕捉療法による悪性神経膠腫の治療効果

Therapy effects of boron neutron capture therapy for malignat glioma

川端信司[1]，宮武伸一[1]，宮田至朗[1]，横山邦夫[1]，
大西恭子[1]，三木義人[1]，黒岩敏彦[1]，
今堀良夫[2]，切畑光統[3]，小野公二[4]

大阪医科大学脳神経外科[1]，CICS（株）[2]，
大阪府立大学　農学部[3]，京都大学原子炉実験所　粒子線腫瘍学[4]

要旨：ホウ素中性子捕捉療法（BNCT）は，理論上腫瘍細胞に選択的照射の可能な粒子線治療である。我々は2002年1月以降，熱外中性子および集積機序の異なる2種類のホウ素化合物（BSH, BPA）を併用した改良型BNCTを用い，50例以上の悪性神経膠腫を治療してきた。改良型BNCTは非開頭で行い，個々の患者でホウ素化合物の腫瘍内集積を考慮し線量計画を行っている。最近では，BPAを700 mg/kgまで増量し，6時間で点滴することで腫瘍内のホウ素濃度を均一化し，照射線量を高めるとともに，新規診断例に対してはX線分割外照射を併用している。新規診断神経膠芽腫で，平均生存期間は診断後23ヵ月（n＝11）であった。選択的照射であるBNCTに外照射を加えることで，新規診断例の治療成績は向上した。また，再発症例においても，他の臨床研究より好成績を示し，予後不良とされるサブグループにおいて有効性が高い傾向が見られた。

Key words：アルファ粒子，ホウ素中性子捕捉療法，悪性神経膠腫

はじめに

悪性神経膠腫はきわめて予後不良の原発性脳腫瘍であり，治療に難渋する最も大きな原因は，腫瘍の浸潤性性格にある。腫瘍の辺縁は明瞭ではなく，細胞レベルでは画像上の造影域を越え，最低でも周囲の正常脳2 cmまでは腫瘍細胞が存在するとされる。そのため，腫瘍の造影域を手術により全摘出しても，再発が必至であり，摘出手術および術後のX線分割外照射・テモゾロミドによる化学療法が，現在の標準的治療法であるが，新規診断例における生存期間中央値は約14ヶ月である[1]。

我々は，前述の浸潤部腫瘍細胞をも選択的に標的可能となる，ホウ素中性子捕捉療法（Boron Neutron Capture Therapy；BNCT, Fig. 1）[2]に注目し，2002年1月以降，52例の悪性脳神経膠腫を治療してきた。我々のBNCTは，熱外中性子を用いた非開頭照射で行い，集積機序の異なる2種類のホウ素化合物（BSH, BPA）を併用したもので，これまでの欧米・本邦での治療プロトコールとは全く異なる改良型である[3-8]。

今回我々は，当施設にて治療を行った，新規

☆論文別刷請求先　〒569-8686　大阪府高槻市大学町2-7
大阪医科大学脳神経外科
川端信司（TEL：072-683-1221, FAX：072-683-4064）
E-mail：neu046@poh.osaka-med.ac.jp

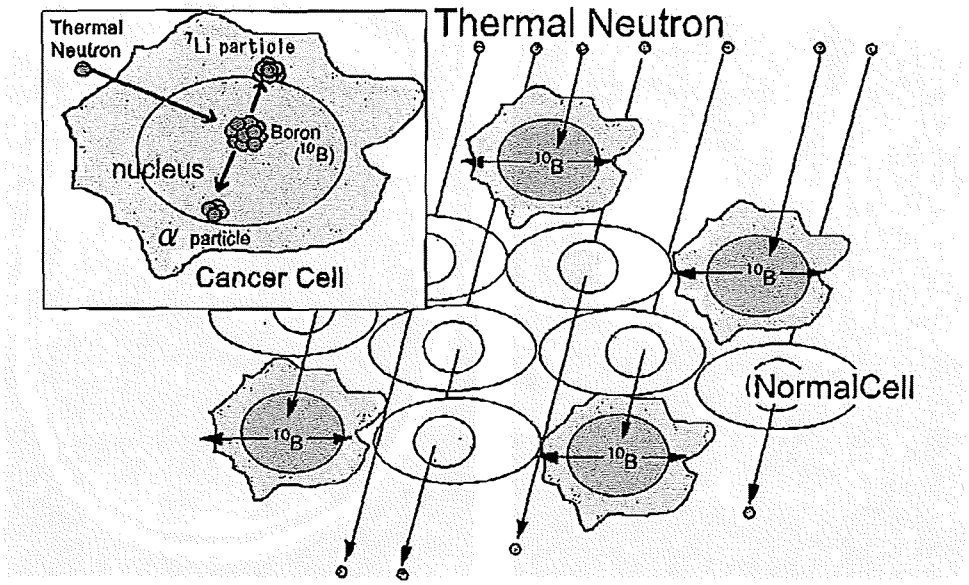

Figure 1 The principle of boron neutron capture therapy (BNCT).
BNCT is a binary approach: A boron-10 (10 B)-labeled compound is administered that delivers high concentrations of 10 B to the target tumor relative to surrounding normal tissues. This is followed by irradiation with thermal neutrons or epithermal neutrons that become thermalized at depth in tissues. The short range (5–9 micrometer) high energy of the alpha and 7 Li particles released from the 10 B (n, alpha) 7 Li neutron capture reaction make tumor selective killing without damage for adjacent normal brain tissue.

診断および再発性の悪性神経膠腫に対する改良型 BNCT の治療成績について解析を加え報告する。

I. 対象と方法

2002 年 1 月から 2007 年 12 月までに，大阪医科大学・脳神経外科で治療を行った悪性神経膠腫は，52 例であった。BNCT は，2 種類のホウ素化合物（BSH および BPA）の併用，熱外中性子による非開頭照射で行い[4]，照射前の^{18}F-BPA PET によるホウ素化合物 BPA の集積 (Fig. 2)[9]および血中ホウ素濃度から，個々の患者の線量計画を行った[3,6,8]。中性子源としては，主として京都大学原子炉実験所（大阪府・熊取）KURRI を利用し，メンテナンスなどの事由で使用不可の期間に関しては日本原子力開発研究機構（茨城県・東海）JRR-4 を利用して行った。本報告では，これらから，元疾患以外の死因によるもの，追跡期間が短期間の生存例，死因が不明または追跡不能例などを除外し解析を行った。新規診断の膠芽腫（WHO grade IV）は 21 例で，これまでに当施設で標準治療（放射線・化学療法）により治療を行った 27 例と比較検討を行った。初発膠芽腫の治療例 21 例中，最近の 11 例では，BNCT 後に 20～30 Gy の X 線分割外照射を加えた。照射線量は，BNCT 時に照射された正常脳の最大線量から算出し，必要に応じて減量した。また，再発悪性神経膠腫では，22 例（膠芽腫 19 例）に BNCT を行い，生存期間に関し解析した。さらに予後因子別のサブ解析として，新規診断例では RTOG（手術，放射線治療）[10]および EORTC（手術，テモゾロミド併用放射線治療）[11]の RPA class 解析の結果と，また再発例に対しては NABTT の RPA class 解析の結果[12]と比較検討を行った。生存解析には Kaplan-Meier 法を用い，Log-rank test にて検定を行った。また Cox 比例ハザードモデルにおける解析を用い，ハザード比を解析した。BNCT 施行後，全例で定期的な MRI 画像による評価を行い，再発または放射線壊死の診断には^{18}F-BPA PET を用い，診断に応じて治療を行った[13]。

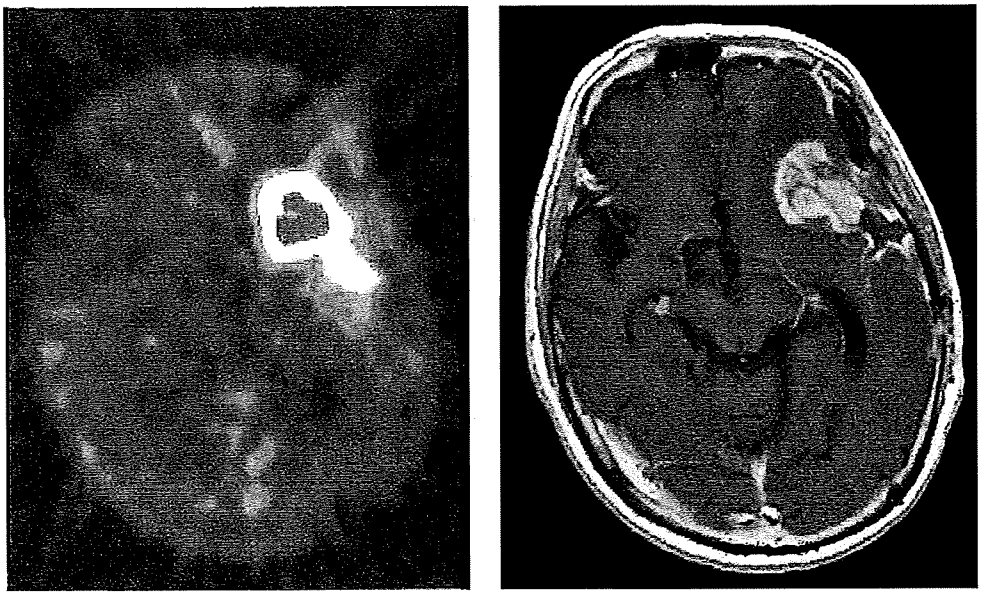

^{18}F BPA PET　　MRI（T 1 Gd）
（T/N：Tumor/Normal Brain ratio）＝7.8

Figure 2 ^{18}F labeled BPA positron emmision tomography (F-BPA PET)
F-BPA PET has been applied for the estimation of the boron compound accumulation prior to BNCT. The tracer is fluororide labelled boron compound. This PET ensures the effectiveness of BNCT. F-BPA accumulates well and distributes precisely in the tumor lesion and the infiltrating tumor zone.

II. 結果

A. 画像所見および合併症・死因

全例で，BNCTによる急性・亜急性の重篤な合併症は経験しなかった。初期の症例で，ホウ素化合物の再結晶化による腎毒性が観察されたが，その後の症例では十分な補液，利尿を行い容易に克服できた。

初発，再発を問わず，全例で画像上の腫瘍の縮小を認め，画像上50%を超える造影域の縮小は67%の症例に認めた[5]。また，BNCT施行後に，ステロイド剤や高浸透圧利尿剤を用いることなく造影域周囲の浮腫は軽減した。死因としては初発，再発ともに髄腔内播種が高率であり，初発例では放射線壊死が死因となった例はなかったが，再発腫瘍に対するBNCT後には22例中3例で放射線壊死が生じた。

B. 生存解析

1. 新規診断膠芽腫に対するBNCT（Fig. 3）

組織診断確定時からの生存期間中央値（MST）は，BNCT群21例で15.6（95% CI；12.2–23.9）ヶ月であり，施設コントロール群（手術，放射線，化学療法）27例の10.3（7.4–13.2）ヶ月を有意に上回った（Fig. 4, Log-rank test, p＝0.0035）。このコントロールを比較対象としたハザードモデルでは，ハザード比0.399（p＝0.0038）であった。また，BNCTに外照射を加えた群11例では，MSTが23.5（10.2－）ヶ月と有意に延長し，コントロールに対するハザード比は0.323（p＝0.004）となった（Fig. 5）。

RTOG RPA class分類では，class IIIが6例，VIが6例，Vが8例，VIは1例であり，それぞれMSTは，23.5, 16.9, 13.2, 9.8ヶ月であった。これはRTOG（手術，放射線治療）でのMST（III；17.9, IV；11.1, V；8.9, VI；4.6）[10]およびEORTC（手術，テモゾロミド併用放射線治療）でのMST（III；21.4, IV；16.3, V；10.3）[11]を上回る結果であった（Fig. 6）。

2. 再発悪性神経膠腫に対するBNCT

BNCTからのMSTは，全22例で10.8（7.3

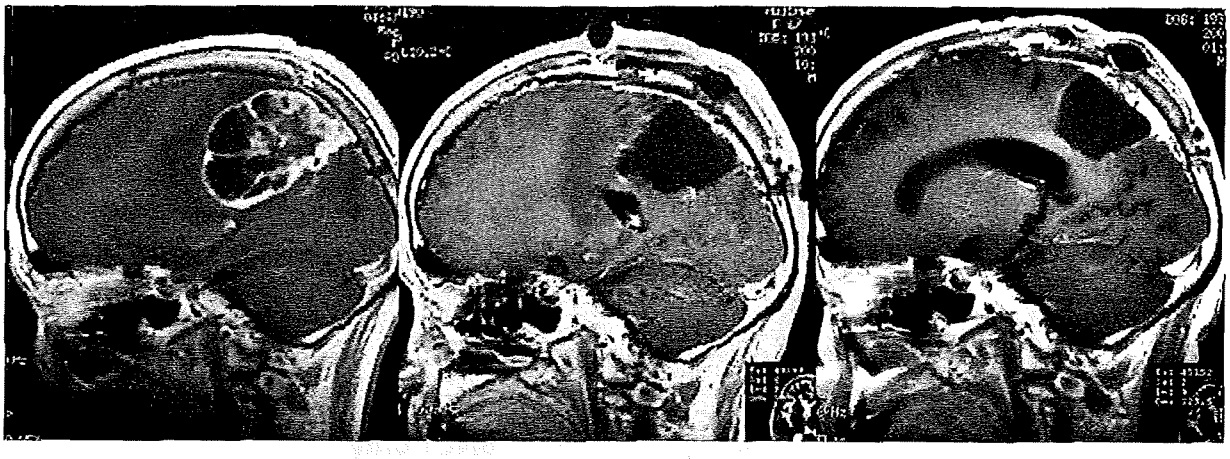

Figure 3 63 y.o., F., Newly diagnoised glioblastoma patient.
She was treated by surgical removal and BNCT followed by external beam X-ray irradiation (2 Gy/day, total 30 Gy). The deepest part of the tumor was 7.5 cm from the scalp in this case. The irradiated minimum tumor dose by BNCT was improved by the air-instilation methods from 18.9 (without air) to 26.9 (with air) Gy-Eq. (left : prior to surgical removal, middle : after surgery, prior to BNCT, right : 44 months after treatment)

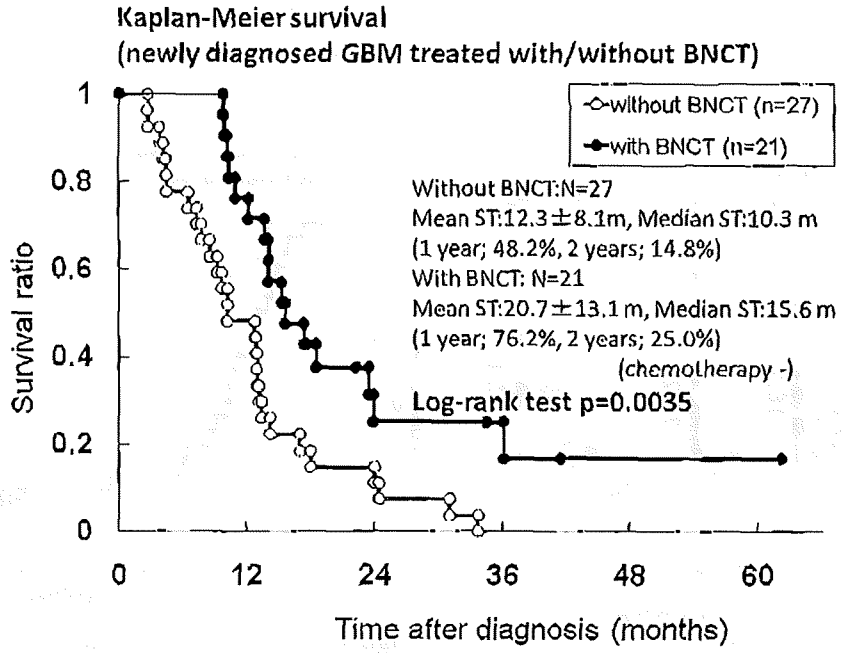

Figure 4 Cumulative data for all newly diagnosed glioblastoma (WHO grade 4, n=21).
This is our recent historical control (gray line) in our institute treated mainly by nitrosourea plus irradiation. The median survival time of BNCT group (black line) is 15.6 months without chemotherapy until tumor progression. There is statistical significance between both group in Log-rank test (p=0.0035).

-12.8) ヶ月であり，再発時の組織診断が膠芽腫であった19例では，9.6 (6.9-11.4) ヶ月であった。これは，NABTTの報告に含まれた全再発悪性神経膠腫のMST (7.0ヶ月，n=310) より良好な結果であった。また，膠芽腫19例の，再発と診断されてからのMSTは19.1 (11.6-23.0) ヶ月であった (Fig. 7)。

NABTTによる再発神経膠腫のRPA class分類において，最も予後不良とされるclass 3が3例 (14%)，class 7は7例 (32%) 含まれ，

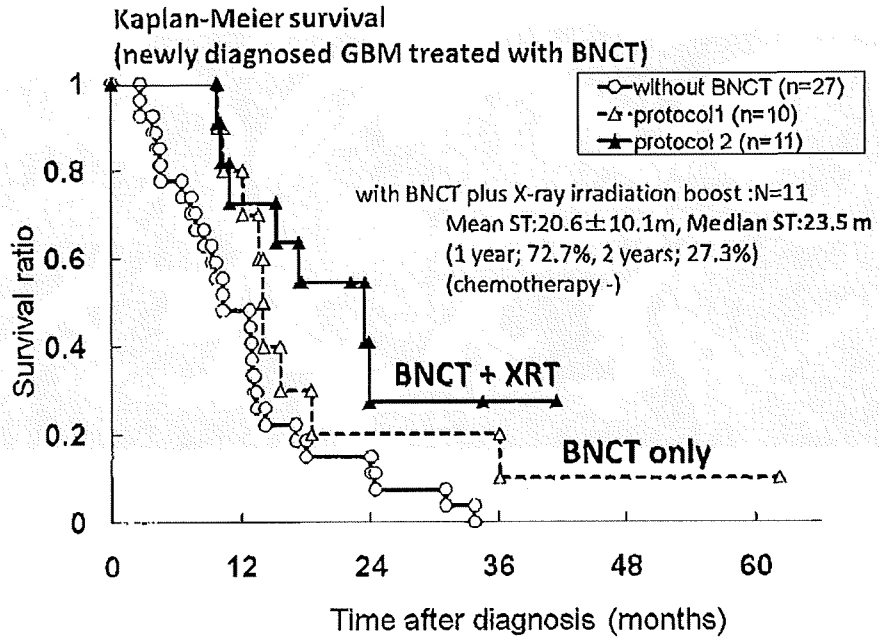

Figure 5 Cumulative data for all newly diagnosed glioblastoma (protocol 1 and 2).
External beam X-ray irradiation (XRT) boost after BNCT (protocol 2, black the median survival time as 23.5 months (vs 14.1 months for BNCT only (protocol 1, dotted line and open triangle)).

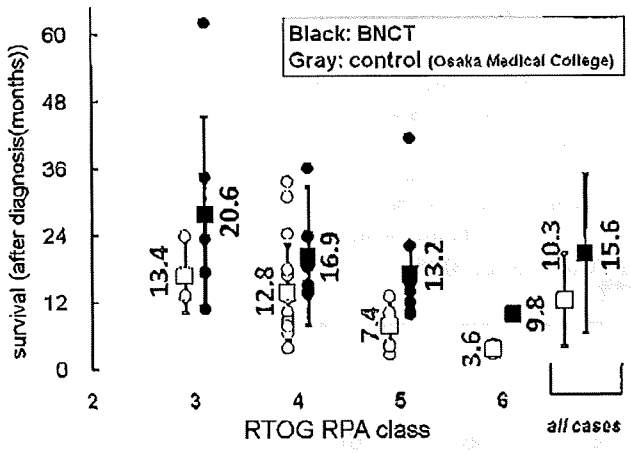

Figure 6 Survival of the corresponding RPA subclasses by RTOG (Curren, 1993).
Mean (square) and individual (circle) survival (bars showing standard deviation) of all cases and each RTOG RPA classes.

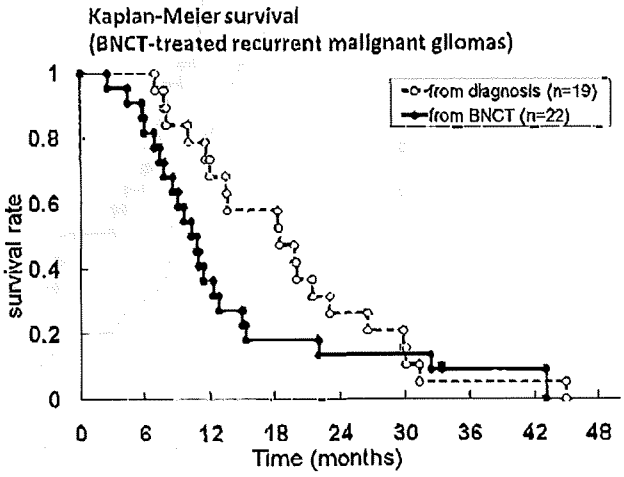

Figure 7 Figure Kaplan-Meier survival curves for the recurrent malignant glioma cases (WHO grade 3&4) treated by BNCT.
A continuous line shows the survival of all patients after BNCT (n=22). A dotted line shows the survival of GBM (on-study histology) after diagnosis of GBM (n=19).

それぞれ BNCT による MST が 11 ヶ月，11 ヶ月と，報告による 3.8, 4.9 ヶ月を大きく上回り (class 3＋7；4.4 (3.6–5.4) ヶ月 vs 9.1 (4.4–11.0) ヶ月)，その他の class においても概ね良好な結果が得られていた。

III. 考察

悪性神経膠腫は，浸潤性の原発性悪性腫瘍であり，手術単独での治癒は望めない。術後の放射線治療は有意に予後を延長させ，近年ではこれにテモゾロミドによる化学療法を加えた治療が標準的に行われているが，その生存期間は約14ヶ月であり，本腫瘍を克服したとは言い難い[1]。

放射線を用いた新しい展望として，ガンマナイフやリニアックによる定位的放射線照射，陽子線，重粒子線および中性子捕捉療法などが現在期待されている。定位的照射に代表される局所高線量照射は，あくまで手術摘出困難な部位における残存腫瘍塊に対して，手術の補助的役割を担う治療法であり，いかに正確にかつ均一に線量を局所に集中させたとしても，浸潤性性格の強い悪性神経膠腫に対して治癒は望めない。これらの線量計画は，画像診断をもとに治療医が行うもので，開頭手術における術者が摘出範囲を決定するのと同様，辺縁部からの再発は免れない。治療範囲の拡大は，外科治療と同様，治療による合併症を高率に招くことになる。放射線治療の中で中性子捕捉療法は，局所高線量という性格を有しながら，腫瘍を細胞レベルで標的とし，正常脳に浸潤した腫瘍細胞をも選択的に治療できるという“細胞選択的粒子線治療”であり，他の放射線治療とは異なる概念を有する画期的な治療法として注目される[2]。

BNCTにより治療を行った，新規診断膠芽腫症例における全生存期間の解析では，中央値が有意差をもって延長し，旧来の標準治療（手術，放射線・化学療法（主としてACNU））の成績より効果があることが示された。今回のBNCT治療群では，初期治療としての化学療法は一切行っておらず，今後BNCTにテモゾロミドを併用することでこの成績はさらに改善しうると考える。さらにハザードモデルでは，コントロール群に対するハザード比は0.4未満で，この数値はランダム化比較検討試験を組む際に，一群あたり20～30症例で有意な差をもって治療効果を示しうる値である。これらの治療群は，何らかのバイアスが存在しうるが，RTOGのRPA class分類による予後因子別の解析を見ても，BNCT治療群は優れた治療成績を示していた。またEORTCによる放射線・テモゾロミドの治療群との比較においても，わずかではあるがすべてのclassでBNCT群が上回っていた。EORTCの報告では，テモゾロミドによる生存期間の延長は，予後良好群ほど大きかったとされるが，我々のBNCTによる治療効果は，予後不良とされるものほど効果が大きい傾向を示した。

悪性神経膠腫では，現時点での初発例に対する治療方針は，前述のごとくであるが[1]，再発例に対する治療方針は，有効とされる標準的なものは一切無く，再発からの生存期間は約6ヶ月である[14,15]。今回我々が示した再発悪性神経膠腫に対する治療成績は，約11ヶ月と良好であるが，比較対象となる治療群は存在せず，この数値のみをもって有効とするには無理がある。そこでこのBNCTによる治療成績を，再発悪性神経膠腫の臨床試験（NABTTの10個のphase I, IIに登録された333例の解析）から得られた予後因子による分類と比較した。これによると，最も予後不良とされたclass 3+7でのMST 4.4（3.6-5.4）ヶ月に対し，BNCT治療群は9.1（4.4-11.0）ヶ月と大きく上回っていた。

我々の改良型BNCTによる治療では，特に予後不良とされるグループにおいて，治療効果が高かった。悪性神経膠腫のごとく浸潤性に発育する腫瘍では，周囲組織への影響が懸念されるが，BNCTは，細胞選択的粒子線治療という特徴から，正常細胞への影響が少なく高線量による放射線治療が可能となるためと考える。

IV. 結語

我々の改良型BNCTは，悪性神経膠腫の新規診断例および再発例に対し，安全に施行しうる有効な治療手段であり，生命予後を改善した。選択的照射であるBNCTにX線外照射を加えることで，新規診断例の治療成績は向上した。また特に，予後不良とされるサブグループ，治療困難例において，有効性が高い傾向が見られた。

文 献

1) Stupp R, Mason WP, van den Bent MJ, et al : Radiotherapy plus concomitant and adjuvant temozolomide for glioblastoma. N Engl J Med 352 : 987–96. 2005.

2) Barth RF, Coderre JA, Vicente MG, et al : Boron neutron capture therapy of cancer : current status and future prospects. Clin Cancer Res 11 : 3987–4002. 2005.

3) Kawabata S, Miyatake S, Kajimoto Y, et al : The early successful treatment of glioblastoma patients with modified boron neutron capture therapy. Report of two cases. J Neurooncol 65 : 159–65. 2003.

4) 川端信司，宮武伸一，梶本宜永ら：グリオーマに対する非開頭ホウ素中性子捕捉療法. Clin Neurosci 21 : 1472–3. 2003.

5) Miyatake S, Kawabata S, Kajimoto Y, et al : Modified boron neutron capture therapy for malignant gliomas performed using epithermal neutron and two boron compounds with different accumulation mechanisms : an efficacy study based on findings on neuroimages. J Neurosurg 103 : 1000–9. 2005.

6) 宮武伸一，川端信司，梶本宜永ら：悪性グリオーマに対する非開頭硼素中性子捕捉療法. 日本臨床 63 : 447–51. 2005.

7) 宮武伸一，横山邦夫，土居 温ら：悪性脳腫瘍に対する硼素中性子捕捉療法〔細胞生物学的 targeting 可能な唯一の放射線治療〕. 定位的放射線治療 10 : 57–65. 2006.

8) 川端信司，宮武伸一：ホウ素中性子捕捉療法. 脳と神経 58 : 1051–9. 2006.

9) Imahori Y, Ueda S, Ohmori Y, et al : Positron emission tomography-based boron neutron capture therapy using boronophenylalanine for high-grade gliomas : part I II. Clin Cancer Res 4 : 1825–41. 1998.

10) Curran WJ, Jr., Scott CB, Horton J, et al : Recursive partitioning analysis of prognostic factors in three Radiation Therapy Oncology Group malignant glioma trials. J Natl Cancer Inst 85 : 704–10. 1993.

11) Mirimanoff RO, Gorlia T, Mason W, et al : Radiotherapy and temozolomide for newly diagnosed glioblastoma : recursive partitioning analysis of the EORTC 26981/22981-NCIC CE 3 phase III randomized trial. J Clin Oncol 24 : 2563–9. 2006.

12) Carson KA, Grossman SA, Fisher JD, et al : Prognostic factors for survival in adult patients with recurrent glioma enrolled onto the new approaches to brain tumor therapy CNS consortium phase I and II clinical trials. J Clin Oncol 25 : 2601–6. 2007.

13) Miyashita M, Miyatake S, Imahori Y, et al : Evaluation of fluoride-labeled boronophenylalanine-PET imaging for the study of radiation effects in patients with glioblastomas. J Neurooncol 89 : 239–46. 2008.

14) Huncharek M, Muscat J : Treatment of recurrent high grade astrocytoma ; results of a systematic review of 1,415 patients. Anticancer research 18 : 1303–11. 1998.

15) Wong ET, Hess KR, Gleason MJ, et al : Outcomes and prognostic factors in recurrent glioma patients enrolled onto phase II clinical trials. J Clin Oncol 17 : 2572–8. 1999.

Therapy effects of boron neutron capture therapy for malignat glioma

Shinji Kawabata[1], Shin-ichi Miyatake[1], Shiro Miyata[1], Kunio Yokoyama[2], Kyoko Onishi[1], Yoshihito Miki[1], Toshihiko Kuroiwa[1], Yoshio Imahori[2], Mitsunori Kirihata[3], Koji Ono[4]

Department of Neurosurgery, Osaka Medical College, Takatsuki, Japan[1], CICS corp. Tokyo, Japan[2], Department of Agriculture, Osaka Prefectural University, Sakai, Japan[3], Particle Radiation Oncology Research Center, Kyoto University Research Reactor Institute, Kumatori, Japan

Boron neutron capture therapy (BNCT) is cell selective particle irradiation based upon the nuclear reaction that occur when non-radioactive boron-10 (^{10}B) is irradiated with low energy neutrons to produce high energy alpha particles.

Since 2002, we have treated >50 cases of malignant gliomas with our modified BNCT utilizing sodium borocaptate (BSH) and boronophenylalanine (BPA) simultaneously. Modified BNCT was carried out without craniotomy using epithermal neutron beam. We used ^{18}F-BPA-PET for almost all the patients who will receive BNCT to estimate the irradiation dose. Recently, we increased the amount of BPA and prolonged the infusion time (700 mg/kg, 6 hours) to give a more homogeneous distribution of boron compounds, even in the infiltrating lesion. Farther more, for the newly diagnosed case, patients were treated with BNCT followed by fractionated X-ray irradiation (XRT) of 20 to 30 Gy.

The median survival time (MST) of newly diagnosed glioblastoma was 21 months (n = 11). With BNCT followed by XRT boost, the MST was significantly extended. Also for the recurrent malignant glioma cases, we showed the survival benefit compare with other clinical studies.

Our modified BNCT protocol showed favorable results of patients with malignant glioma not only for those with good prognoses but also for those with poor prognoses.

Key words : alpha particle, boron neutron capture therapy, malignant glioma

J Neurosurg 112:50–56, 2010

Phase II study of ifosfamide, carboplatin, and etoposide in patients with a first recurrence of glioblastoma multiforme

Clinical article

Tomokazu Aoki, M.D., Ph.D.,[1] Tomohiko Mizutani, M.D., Ph.D.,[7] Kuniharu Nojima, M.D., Ph.D.,[8] Takehisa Takagi, M.D., Ph.D.,[2] Ryosuke Okumura, M.D., Ph.D.,[3] Yoshiaki Yuba, M.D.,[4] Tetsuya Ueba, M.D., Ph.D.,[5] Jun A. Takahashi, M.D., Ph.D.,[1] Shin-Ichi Miyatake, M.D., Ph.D.,[6] Kazuhiko Nozaki, M.D., Ph.D.,[9] Waro Taki, M.D., Ph.D.,[10] and Masao Matsutani, M.D., Ph.D.[11]

Departments of [1]Neurosurgery, [2]Radiation Oncology, [3]Radiology, [4]Pathology, Kitano Hospital Medical Research Institute; [5]Department of Neurosurgery, Kishiwada City Hospital; [6]Department of Neurosurgery, Osaka Medical College, Osaka; [7]Department of Neurosurgery, Hyogo Prefectural Amagasaki Hospital; [8]Department of Neurosurgery, Ako City Hospital, Hyogo; [9]Department of Neurosurgery, Shiga University of Medical Science, Shiga; [10]Department of Neurosurgery, Faculty of Medicine, Mie University, Mie; [11]Department of Neurosurgery, Saitama Medical University International Medical Center, Saitama, Japan

Object. The prognosis of recurrent glioblastoma multiforme (GBM) remains unsatisfactory. The authors conducted a Phase II study of ifosfamide, carboplatin, and etoposide (ICE) for a first recurrence of GBM to determine whether it prolonged a patient's good-quality life.

Methods. This trial was an open-label, single-center Phase II study. Forty-two patients with a first GBM relapse after surgery followed by standard radiotherapy (60 Gy) and first-line temozolomide- or nimustine-based chemotherapy were eligible to participate. The primary end point was progression-free survival at 6 months after the ICE treatment (PFS-6), and secondary end points were response rate, toxicity, and overall survival. Chemotherapy consisted of ifosfamide (1000 mg/m^2 on Days 1, 2, and 3), carboplatin (110 mg/m^2 on Day 1), etoposide (100 mg/m^2 on Days 1, 2, and 3), every 6 weeks.

Results. Progression-free survival at 6 months after ICE treatment was 35% (95% CI 22–50%). The median duration of PFS was 17 weeks (95% CI 10–24 weeks). The response rate was 25% (95% CI 9–34%). Adverse events were generally mild and consisted mainly of alopecia.

Conclusions. This regimen was well tolerated and has some activity and could be one of the options for patients with recurrent GBM. *(DOI: 10.3171/2009.5.JNS081738)*

Key Words • **glioblastoma multiforme** • **chemotherapy** • **ifosfamide** • **carboplatin** • **etoposide**

Glioblastoma multiforme is one of the most devastating malignancies, destroying important cognitive functions in the brain, altering the personalities of humans, and leading to death. Standard treatment of a newly diagnosed GBM usually consists of cytoreductive surgery followed by conventional radiotherapy concomitant with temozolomide chemotherapy.[1,22] Gliadel wafers also have been used in patients with GBM.[29] Despite the administration of multimodal treatments, this tumor always recurs no more than 1 or 2 years later. Unfortunately, we have no established second-line treatments once the tumor progresses.[9]

As shown in a published database of Phase II trials that included 225 patients with recurrent GBM, the benefit from chemotherapy in such patients is very limited.[31] The median duration of PFS is 9 weeks, and PFS at 6 months (PFS-6) is 15%, meaning that 15% of patients survive without tumor progression by 6 months after treatment. Several chemotherapeutic or biological agents may palliate patients but produce only a minimal increase in survival, although dose-intensified temozolomide or bevacizumab has shown promising effects.[24,26]

Carboplatin has demonstrated activity against malignant brain tumors.[33] Etoposide, a semisynthetic derivative of podophyllotoxin, has shown synergistic activity with cisplatin.[16] Ifosfamide is an alkylating agent that has

Abbreviations used in this paper: CR = complete response; GBM = glioblastoma multiforme; ICE = ifosfamide-carboplatin-etoposide; KPS = Karnofsky Performance Scale; MGMT = O^6-methylguanine-DNA methyltransferase; NCI = National Cancer Institute; NR = no response; PFS = progression-free survival; PR = partial response.

demonstrated an increased therapeutic effect in a variety of refractory solid tumors.[34] The ifosfamide-carboplatin-etoposide (ICE) combination has demonstrated a therapeutic effect in a broad range of malignancies, even after the failure of previous chemotherapy.[19]

A Phase II study of the ICE regimen in patients with recurrent malignant GBMs has been conducted with interesting results.[20] Carboplatin and etoposide were both given at a dose of 75–100 mg/m^2/day for 3 days, whereas a dose of ifosfamide ranging from 750 to 1500 mg/m^2/day was administered for 3 days. This regimen was repeated every 4 weeks. The PFS-6 was ~ 30% and the response rate was 28%, but the hematological toxicity was not acceptable. Recurrent malignant GBMs are refractory and ultimately incurable. Long-term tumor stabilization with low toxicity is important in the management of malignant lesions.[23] We performed a feasibility study of a lower-dose ICE regimen to confirm whether its safety and efficacy were acceptable. A feasibility study in 15 patients with malignant GBMs showed a response rate of 45% and Grade 3 or 4 toxicities of 8% (unpublished data); therefore, we initiated a Phase II study of a lower-dose regimen for further evaluation.

Methods

Eligibility for Study Participation

Patients enrolled in the study had a first relapse of supratentorial GBM previously treated with surgery, conventional radiotherapy (60 Gy), and a first-line nitrosourea-based[2] or temozolomide-based chemotherapy. Tumor progression was confirmed on Gd MR imaging. If radiation necrosis or pseudoprogression was suspected, spectroscopic MR imaging was performed to confirm the presence of viable cells. If mainly necrosis was noted in those who underwent repeat surgery for a recurrence, adjuvant chemotherapy was continued. Patients were required to be at least 18 years old, have a KPS score ≥ 60, and have a life expectancy > 12 weeks. An interval > 12 weeks from the completion of radiotherapy, > 4 weeks from prior chemotherapy (6 weeks from a nitrosourea-based regimen), and > 2 weeks from surgery had to have elapsed for the patient to be eligible for study enrollment. Adequate laboratory values were also required, including a neutrophil count ≥ 1500/ml^3, platelet count ≥ 100,000/mm^3, transaminase and alkaline phosphatase levels < 3 times the upper limit of laboratory normal, and serum creatinine and bilirubin levels < 1.5 times the upper limit of laboratory normal. In addition, patients could not be pregnant, have an uncontrolled infection, or have had any prior malignancy. All patients signed informed consent according to the principles of the Declaration of Helsinki and the rules of good clinical practice. The institutional review board of Kitano Hospital, Japan, approved the protocol.

Patient Characteristics

Between March 2002 and February 2005, 42 patients were prospectively enrolled in the study. Their median age was 55 years (range 21–70 years), and 57% (24 of 42 patients) were men (Table 1). Fifty-five percent (23 of 42) of the patients had a KPS score ≥ 80. All patients had undergone surgical interventions at the time of the initial diagnosis of GBM. Furthermore, all patients had undergone conventional radiotherapy (2.0 Gy per fraction 5 times a week, total dose 60 Gy), followed by a first-line chemotherapy regimen consisting of a nimustine (ACNU)-based regimen[2] in 24 patients and temozolomide in 18 patients. The median time from the initial diagnosis to first relapse was 39 weeks (range 12–98 weeks). Between the patients who had been on a temozolomide regimen and those on a nimustine regimen, there was no significant difference in the prognostic factors (age, sex, and KPS score) and the time from first diagnosis to study enrollment. Salvage surgery at the first recurrence before ICE treatment was performed in 14 patients (33%); on the basis of MR imaging results, the extent of resection was considered gross total in 10 patients and partial in 4. At enrollment 35 of 42 patients were taking antiepileptic prophylaxis without enzyme-inducing properties (valproic acid); 7 patients were on antiepileptic prophylactic enzyme-inducing drugs (phenytoin in 4 cases, phenobarbital in 2, and carbamazepine in 2).

Treatment Regimen

Chemotherapy consisted of ifosfamide (1000 mg/m^2 on treatment Days 1, 2, and 3), carboplatin (110 mg/m^2 on treatment Day 1), and etoposide (100 mg/m^2 on treatment Days 1, 2, and 3). This combination was intravenously administered and repeated every 6 weeks until tumor progression, provided that all hematological toxicities from the previous course had resolved to a Grade 2 or lower (NCI common toxicity criteria, version 3.0) and all nonhematological toxicities had recovered to either Grade 0 or 1. If enough recovery had not occurred, the subsequent course was delayed until these criteria were met; a delay of up to 2 weeks was allowed. No dose escalation was allowed. Dose reduction for toxicity was allowed—a 30% reduction for all drugs—but only 2 dose reductions were permitted. Patients having Grade 3 toxicity of any type after 2 dose reductions were excluded from the study. Ondansetron was given to all patients before administration of the chemotherapy regimen to prevent nausea and vomiting.

Schering-Plough Pharmaceuticals kindly supplied the temozolomide through a compassionate use program, as the Japanese administrative agency only approved temozolomide in September 2006.

Response Evaluation

Response was assessed using a modification of the Macdonald criteria.[18] We compared baseline contrast-enhanced MR images obtained in a week before every course of chemotherapy, while also considering any changes on the neurological examination and the dose of steroids. In brief, CR was defined as the disappearance of all enhanced tumors at least 1 month after they had appeared on the last MR image obtained, with no corticosteroids and no neurological deterioration. Partial response was defined as a > 50% reduction in lesion size

TABLE 1: Summary of characteristics in 42 patients with recurrent GBM

Parameter	No. (%)
age in yrs	
median	55
range	21–70
<50	14 (33)
≥50	28 (67)
sex	
M	24 (57)
F	18 (43)
KPS score	
100	4 (12)
90	9 (26)
80	10 (33)
70	6 (19)
60	3 (10)
time from 1st diagnosis to study enrollment (wks)	
median	39
range	12–98
antiepileptic prophylaxis w/ enzyme-inducing drug	7 (17)
prior treatment at 1st relapse	
salvage surgery	
gross-total resection	10 (24)
partial resection	4 (10)
no surgery	28 (66)
chemotherapy regimens	
temozolomide	18 (43)
nimustine-based regimen	24 (57)

(the product of the largest perpendicular diameters). This response had to be maintained for at least 1 month without either neurological deterioration or an increased dose of corticosteroids. No response was defined as no change in tumor size for a minimum interval of 4 weeks or a change in tumor size after 1 month that did not qualify as a CR, PR, or progressive disease. Progressive disease was defined by the following: any new tumor or a > 25% increase in lesion size, a deterioration in the patient's neurological status, or a stable neurological status on an increased dose of steroids. Unequivocal evidence of recurrence or progression of the disease on Gd MR imaging was also required; acceptable evidence was disease progression on 2 subsequent MR images separated by at least 1 month. A multidisciplinary team consisting of a neurosurgeon, a neuroradiologist, a neurooncologist, and a radiotherapist evaluated the images.

Treatment Toxicity

Toxicity monitoring was performed in patients on all treatment cycles, according to the NCI common toxicity criteria (version 3.0) (http://ctep.cancer.gov/protocolDevelopment/electronic_applications/docs/ctcaev3.pdf). A physical examination, complete blood count, urinalysis, and biochemistry profile were performed every cycle. Weekly hematological tests and serum chemistries were also required.

Statistical Considerations

The primary end point of this study was the percentage of patients alive and progression free at 6 months (PFS-6). Secondary end points included the percentage of patients who were progression free at 3, 12, and 18 months; tumor response to treatment; overall survival; and time to disease progression. The regimen would be considered a success if at least 30% of enrolled patients responded to it, whereas the regimen would be considered ineffective if a success rate ≤ 10% was observed. In the North Central Cancer Treatment Group (NCCTG) database of patients with recurrent GBMs, the PFS-6 was 10%.[31] Our design used 33 patients and had an alpha level of 0.04 and a power of 0.89 for detecting a true success probability of 30%. The original sample size of the trial was 37 (33 patients with 4 additional patients in case of drop-outs), and 42 patients were accrued initially.

The time to progression was defined as the time from study entry to disease progression. Patients who died were considered to have disease progression at the time of death until there was documented evidence that no progression had occurred before death. Overall survival was defined as the time from study entry to death from any cause. Patients who did not die or whose tumor did not progress were censored at the last known follow-up.

Results

The median follow-up period was 13.2 months (range 1.5–22.4 months).

Treatment Responses

Only 36 patients could be assessed for a treatment response because 5 patients underwent almost total resection at a salvage surgery and 1 patient died of a pulmonary embolism during the 1st month of treatment before any response could be evaluated. There was 1 CR (3%) and 8 PRs (22%) to the ICE treatment (Table 2). The overall response rate (CR + PR) was 25% (9 of 36 patients, 95% CI 12–37%). The median duration of disease stabilization in 18 patients was 21 weeks (range 6–69 weeks). The median duration of the overall response rate (CR + PR) was 25 weeks (range 8–71 weeks). All responding patients were taking either a stable dose of or no corticosteroids at the time of the best response. The rate of stable disease was 50% (95% CI 39–62%).

Disease Progression

Considering all 42 enrolled patients (Fig. 1), the median time to tumor progression was 16.2 weeks (95% CI 12.4–27.3 weeks). Progression-free survival at 6 and 12 months after ICE treatment were 35% (95% CI 22–43%) and 7% (95% CI 3–15%), respectively. On univariate analysis, there was no difference in the possibility of progression based on surgical treatment at relapse ($p = 0.55$), the extent of surgery ($p = 0.31$), prior nitrosourea-based chemotherapy ($p = 0.46$), patient age ($p = 0.33$), or KPS